

AD-A191 859

STRUCTURE AND REFINEMENT OF ORDERED AROMATIC
HETEROCYCLIC POLYMERS BY DIF. (U) BAYTON UNIV ON DEPT
OF CHEMISTRY A U FRATTINI FEB 88 AFOSR-YR-88-0049
AFOSR-84-0364

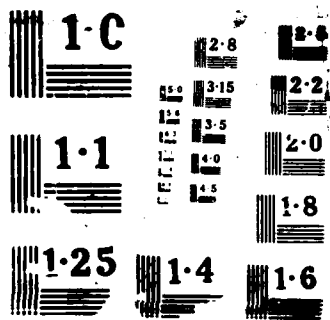
1/1

UNCLASSIFIED

F/C 7/6

NL

END
DATE
FILMED
5 84



unclassified

2

AD-A191 859

DOCUMENTATION PAGE

Form Approved OMB No. 0704-0188

1a. REPORT SECURITY CLASSIFICATION unclassified			1b. RESTRICTIVE MARKINGS DTIC FILE COPY	
2a. SECURITY CLASSIFICATION AUTHORITY			3. DISTRIBUTION / AVAILABILITY OF REPORT Approved for Public Release, distribution unlimited	
2b. DECLASSIFICATION / DOWNGRADING SCHEDULE			5. MONITORING ORGANIZATION REPORT NUMBER(S) AFOSR-TR- 88-0049	
4. PERFORMING ORGANIZATION REPORT NUMBER(S)				
6a. NAME OF PERFORMING ORGANIZATION Dept. of Chemistry University of Dayton		6b. OFFICE SYMBOL (if applicable)	7a. NAME OF MONITORING ORGANIZATION AFOSR/NC	
6c. ADDRESS (City, State, and ZIP Code) 300 College Park Ave. Dayton, Ohio 45469			7b. ADDRESS (City, State, and ZIP Code) Bldg 410 Bolling AFB DC 20332-6448	
8a. NAME OF FUNDING / SPONSORING ORGANIZATION AFOSR		8b. OFFICE SYMBOL (if applicable) NC	9. PROCUREMENT INSTRUMENT IDENTIFICATION NUMBER AFOSR-84-0364	
8c. ADDRESS (City, State, and ZIP Code) Bldg 410 Bolling AFB DC 20332-6448			10. SOURCE OF FUNDING NUMBERS	
	PROGRAM ELEMENT NO. 61102F	PROJECT NO. 2303	TASK NO. A3	WORK UNIT ACCESSION NO.
11. TITLE (Include Security Classification) Structure and Refinement of Ordered Aromatic Heterocyclic Polymers by Diffraction Methods: <i>Application of results to Electro-Optic Phenomena</i>				
12. PERSONAL AUTHOR(S) Fratini, Albert V.				
13a. TYPE OF REPORT Final Report		13b. TIME COVERED FROM 9/30/84 TO 10/31/87	14. DATE OF REPORT (Year, Month, Day) February 1988	15. PAGE COUNT iv + 58
16. SUPPLEMENTARY NOTATION				
17. COSATI CODES			18. SUBJECT TERMS (Continue on reverse if necessary and identify by block number)	
FIELD	GROUP	SUB-GROUP	ordered polymers, fiber structure, polybenzothiazoles, rigid rod polymers, linked-atom least-squares PBT ladder polymer, polybenzoxazoles PBO	
07	04			
11	04			
19. ABSTRACT (Continue on reverse if necessary and identify by block number) The polymer structure determination and refinement of flexible coil poly-2,5-benzoxazole (ABPBO) and poly-2,6-benzothiazole (ABPBT) were performed. Refinement of the unit cell structure of poly(p-phenylene benzobisoxazole) (PBO) and poly(p-phenylene benzobisthiazole) (PBT) in a nonprimitive monoclinic unit cell was carried out in a similar fashion. Initial structural models were derived from x-ray studies of model compounds. Experimental structure factors were incorporated into the Linked-Atom Least-Squares (LALS) refinement method. The Structure of the benzimidazoisoquinoline ladder polymer (BBL) was also investigated. BBL shows potential as an organic conducting polymer. The feasibility of BBL and similar systems to act as conducting polymers requires accurate molecular structure and crystallographic data for an understanding of the mechanical, optical and electro-optic properties. Possible <i>(Keyman...)</i>				
20. DISTRIBUTION / AVAILABILITY OF ABSTRACT <input checked="" type="checkbox"/> UNCLASSIFIED/UNLIMITED <input checked="" type="checkbox"/> SAME AS RPT <input type="checkbox"/> DTIC USERS			21. ABSTRACT SECURITY CLASSIFICATION Unclassified	
22a. NAME OF RESPONSIBLE INDIVIDUAL Major Larry P. Davis			22b. TELEPHONE (Include Area Code) (202) 767-4963	22c. OFFICE SYMBOL NC

DTIC ELECTED
FEB 25 1988

unclassified

SECURITY CLASSIFICATION OF THIS PAGE

11. Title: Application of Results to Electro-Optic Phenomena.

18. Subject Terms: ABPBO ABPBT

19. Abstract: dopant sites were identified in BBL. Research is presented which describes how modifying the chemical structure of PBT by attaching bulky benzothiazole groups to the polymer backbone affects the conformation and packing of polymer chains. The single crystal structure determination of several model compounds which contain pendant benzothiazole, benzoxazole and benzimidazole groups attached to the phenylene ring is reported.

STRUCTURE AND REFINEMENT OF ORDERED
 AROMATIC HETEROCYCLIC POLYMERS BY DIFFRACTION METHODS:
 APPLICATION OF RESULTS TO ELECTRO-OPTIC PHENOMENA

Albert V. Fratini
 Department of chemistry
 University of Dayton
 Dayton, Ohio 45469

Final Report, September 30, 1984 - October 31, 1987

Grant AFOSR-84-0364

Air Force Office of Scientific Research

February, 1988

Accession For	
NTIS GRA&I	<input checked="" type="checkbox"/>
DTIC TAB	<input type="checkbox"/>
Unannounced	<input type="checkbox"/>
Justification	
By _____	
Distribution/	
Availability Codes	
Dist	Avail and/or Special
A-1	

98 2 21 12P

Approved for public release,
 distribution unlimited

FOREWORD

This report was prepared at the Department of Chemistry of the University of Dayton, under Grant AFOSR-84-0364. The research discussed herein was administered under the direction of the Air Force Office of Scientific Research, Bolling Air Base, Washington, D.C., 20332.

The research was performed in the Department of Chemistry at the University of Dayton and in the Materials Laboratory, Air Force Wright Aeronautical Laboratories, Wright-Patterson Air Force Base, under the direction of Dr. Albert V. Fratini, the principal investigator. The technical assistance of M. Anater, Dr. K. Baker, G. Borchers, E. Cross, C. George, Dr. H. Knachel, J. Plashke, and M. Sturtevant is gratefully acknowledged.

The report covers work performed between September 30, 1984, and October 31, 1987.

A. RESEARCH OBJECTIVES

The research was carried out to obtain detailed structural information on the rodlike and stiff-chain, aromatic heterocyclic class of polymers. The attainment, in these polymers, of mechanical and thermal oxidative properties comparable or superior to those obtained with fiber reinforced composites has been demonstrated by scientists associated with the Ordered Polymer Research Program in the Materials Laboratory at Wright-Patterson Air Force Base. It is known that heat treatment under tension brings about significant enhancement of the tensile properties of these polymers. The effect of processing conditions (i.e., dope concentration, extrusion temperature, heat treatment temperature) on the resultant polymer structure is consequently of prime importance.

A specific area of research was the polymer structure determination and refinement of the flexible coil poly-2,5-benzoxazoles (ABPBO), poly-2,6-benzothiazoles (ABPBT), and poly-2,5(6)benzimidazoles (ABPBI). Initial structural models for ABPBX were devised employing molecular parameters derived from single crystal x-ray studies of model compounds. Experimental structure factor amplitudes were obtained from x-ray and electron diffraction measurements and subsequently incorporated into the Linked-Atom Least-Squares (LALS) refinement scheme.

Another goal of this research was to examine by diffraction methods the unit cell structure and the possible molecular

conformations of the benzimidazoisoquinoline ladder polymer (BBL), which shows potential as an organic conducting polymer. Of interest was an understanding at the molecular level of the characteristic mechanical, optical and electro-optic, and processing properties of these pi-electron materials. Knowledge of intermolecular interaction energies and electronic band gaps, all of which require accurate molecular and crystallographic data, have a bearing on the feasibility of BBL and similar systems to act as conducting polymers.

The addition of bulky benzothiazole groups to PBT backbone enhances the solvation characteristics of the polymer without imposing restrictions on the processing variables. Our effort has been to determine how changing the chemical structure of PBT affects the conformation and packing of polymer chains and in turn the observed tensile, compressive, and optical properties.

The single crystal structure determination of several model compounds capable of providing accurate structural data were performed. Of particular interest are those compounds which contain pendant benzothiazole, benzoxazole and benzimidazole groups attached to a phenylene segment.

B. STATUS OF RESEARCH

LALS Refinement Procedure: The applicability of the LALS refinement method to high performance fibers has been reported. We have investigated oriented fibers of semi-crystalline

poly(aryl-ether-ether-ketone) (PEEK) - an engineering thermoplastic polymer as well as a flexible chain matrix for rigid rod polymers such as PBT - in order to gain additional experience with LALS as a structural tool (see Reprint 1). Fibers with percent crystallinities of the order of 30 percent were studied. The results support previous findings indicating that space group $Pbcn$ is a valid representation for the three-dimensional structure of oriented PEEK fibers. It is concluded from the refinement of the two-ring unit that a single torsion angle can describe the conformation of the six-ring crystallographic repeat unit.

ABPBX Polymers: The crystalline structure of oriented fibers of ABPBO and ABPBT have been investigated (see Reprint 2). Both unit cells are metrically orthorhombic. In each structure the fiber repeat unit consists of a dimer arranged in a planar zig-zag conformation. The torsion angle between ring systems and the orientation of chains in the unit cell were refined using measured diffraction intensities taken from fiber rotation patterns.

A static disorder model for ABPBO in which fifty percent of the chains have their chain directions reversed yielded a better fit between calculated and measured structure factors. Welsh and Mark have reported torsional energy minima at 0° and 180° , which is in agreement with this work. They also report a barrier to free rotation about the single rotatable bond of about 1.6 kcal/mole. Thus the observed enhancement in molecular ordering following heat treatment presumably is associated with this type of motion.

PBX Polymers: The primary factors contributing to superior tensile properties of the rigid rod polymers are high axial order and orientation, in conjunction with perfection of lateral structure. We have determined the dimensions of the non-primitive unit cell and have refined the structure of rodlike poly(p-phenylene benzobisthiazole) (PBT) and poly(p-phenylene benzobisoxazole) (PBO) (see Abstracts 1 and 2). A publication describing this work is in preparation. The non-primitive unit cells relieve the overshoot H --- H contacts, inherently part of the primitive cell, by allowing the repelling hydrogen atoms on adjacent chains to no longer be in perfect registry. Three-dimensional order in the form of off-axis Bragg maxima was noted on fiber rotation and zero layer precession photographs of PBT and PBO. Heat treatment also sharpened the rather broad equatorial and diffuse meridional reflections, indicating improved molecular order.

BBL Ladder Polymer: There are several properties which make the ladder polymer, poly[(7-oxo-7, 10H-benz[de]-imidazo [4',5':5,6] benzimidazo [2,1-a] isoquinoline-3,4:10,11-tetrayl)-10 carbonyl] (BBL) of immediate interest. It can resist thermo-oxidative degradation at temperatures as high as 500°C in air (700°C in nitrogen atmosphere). Films also become semi-conducting after doping with 98% H₂SO₄ and other dopants. A high degree of order is attainable when the polymer is processed from liquid crystalline solutions containing strong acids.

The structure of as-spun fibers has been investigated and our findings substantiate earlier work which indicates that in the

solid state BBL exhibits a fully conjugated and layered unit cell structure. An orthorhombic unit cell produced the best correlation between observed and calculated d-spacings. The cell dimensions are $a = 8.29(6)$, $b = 3.38(1)$, $c = 11.97(3)$ Å. The calculated density based on one chain per cell is 1.65 g/cm^3 , which is consistent with the measured fiber density of 1.59 g cm^{-3} . The relatively high density is in accord with the observation that BBL is highly ordered and uniformly packed. The refinement of the structure involved the rotation of planar molecules about the c axis (fiber axis). The molecules were initially positioned in the (010) face; intra- and intermolecular contacts were then computed, followed by a comparison of calculated and observed structure factors. The structure of the chemical repeat unit was derived from model compound structures, namely 2,6-diphenyl benzodiimidazobenzene (PDIAB) (see Publ. 1). Only one of four possible starting isomeric conformations for BBL was investigated. Three equatorial and one-off axis reflections were used in the refinement scheme. The final rotation angle (setting angle) about the z -axis was 5° . The shortest contacts (1.76 and 1.79 Å) were between nonbonded hydrogen atoms. Potential sites for dopant ions in the unit cell were identified; they involved hydrogen bonding to carbonyl and imidazole functions on the polymer backbone. Further work awaits the processing of heat treated fibers which possess improved three-dimensional order.

Pendant PBT Polymers (PPBT): Wide angle x-ray diffraction patterns of as-spun and heat treated specimens of PPBT revealed

additional diffraction peaks as compared to PBT. The origin of the 12 \AA reflection along the equator, which is observed in as-spun fibers but is absent in heat treated samples, can be explained in terms of nematic type packing of PPBT chains. The identity period along the fiber axis (24.9 \AA) is twice the value found in PBT (12.4 \AA). While the unit cell structure of PPBT preserves some features of the PBT lattice, the introduction of defects into a superlattice structure is still necessary to explain the additional diffraction peaks. Various packing models have been examined involving a monoclinic unit cell of dimensions $a = 16.61$, $b = 9.09$, $c = 24.9 \text{ \AA}$ and $\gamma = 95.2^\circ$. The observed fiber density measured in mixed solvents was 1.53 g cm^{-3} , which is less than the value found for PBT (1.59 g cm^{-3}). Considering just the intramolecular interactions, the conformational angles for the chemical repeat unit were obtained from energy minimization calculations on one repeat unit.

Model Compound Structures: Single crystal crystallographic methods were used in the structure determination of two model compounds (see Preprint 1). These compounds are relevant to the structure determination of ordered polymers which contain benzoxazole, benzothiazole and benzimidazole pendant groups.

Refinement of the structure of PEEK fibre in an orthorhombic unit cell

A. V. Fratini* and E. M. Cross

Department of Chemistry, University of Dayton, Dayton, Ohio 45469, USA

and R. B. Whitaker

Monsanto Research Corporation, Mound Laboratory, Miamisburg, Ohio 45342, USA

and W. W. Adams

Materials Laboratory, Wright-Patterson Air Force Base, Ohio 45433, USA

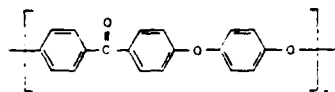
(Received 24 July 1985)

The crystalline structure of oriented fibres of poly(ether-ether-ketone) (PEEK) has been analysed by X-ray diffraction and refined by the 'linked-atom least-squares' procedure. The conformation of chains, consisting of a six-aryl ring unit, is approximated by the refinement of a two-aryl ring unit within the orthorhombic unit subcell with dimensions: $a = 7.83 \pm 0.02$ Å, $b = 5.94 \pm 0.01$ Å and $c = 9.86 \pm 0.04$ Å. Certain constraints imposed by Pbcn space group symmetry are relaxed during refinement. The results of the two-ring refinement indicate that a single torsion angle can be used to describe the conformation of the six-ring unit. The torsion angle corresponds to the average tilt of the phenylene rings out of the (100) face, and the best fit is obtained with an angle of 37° . The simulated powder diffraction pattern based on the atomic coordinates of the six-ring unit matches very closely previously reported patterns for a variety of PEEK specimens. The analysis supports and extends to oriented fibres the previously reported finding that space group Pbcn is a valid representation for the structure of PEEK.

(Keywords: poly(ether-ether-ketone); X-ray diffraction; fibre patterns; structural refinement; powder pattern)

INTRODUCTION

Crystalline and amorphous poly(aryl-ether-ether-ketone) (PEEK), having the following chemical composition



is a promising engineering thermoplastic polymer with important structural applications. Recent papers have reported the unit cell structure of various PEEK specimens, including oriented heat treated fibres.¹⁻⁴ These papers point to the similarity of the unit cell dimensions and chain conformation as confirming evidence that the Pbcn space group and unit cell structure for poly(phenylene oxide) (PPO) is a good model for PEEK.⁵ The manner in which the chains pack in the crystallite regions is, however, an aspect of the PEEK structure that has been somewhat more difficult to characterize. As depicted in Figure 1, the *c*-axis fibre repeat extends over two aryl units, while the chemical repeat encompasses three aryl units, suggesting a disordered structure in which the ether and ketone groups are crystallographically equivalent. The disorder might be viewed in terms of an irregular sequence of ketone and ether linkage groups along the polymer chain. Additional axial chain stacking irregularity would further complicate the disorder picture. Another viewpoint assumes no

inherent irregularity in the sequence of linkage groups, but is based on an irregular packing of neighbouring chains. Depending on factors such as the degree of crystallinity and density, the arrangement of neighbouring chains could range from one of random stacking of adjacent ketone and ether groups to one in which the stacking is more perfect.

The paper reports the refinement of the structure of crystalline PEEK fibre in an orthorhombic unit cell using the 'linked-atom least-squares' (LALS) technique.⁶ Where possible, the symmetry constraints of space group Pbcn have been maintained. The conformation and packing of chains are approximated by refinement of the two-ring unit within a unit subcell. The volume of the subcell is one-third the volume of the Pbcn unit cell. It is concluded from the results of the refinement of the two-ring unit that a single torsion angle can be used to describe the conformation of the six-ring unit.

EXPERIMENTAL

Materials

Heat treated monofilament of diameter 0.2 mm was obtained from Albany International, Homer, New York. The density of the fibre was measured by flotation in a toluene-carbon tetrachloride mixture, and also by the buoyancy method by immersing the sample in toluene.

X-ray photography

X-ray diffraction photographs were obtained from precession and 28.6 mm radius single crystal cylindrical

* To whom correspondence should be addressed.

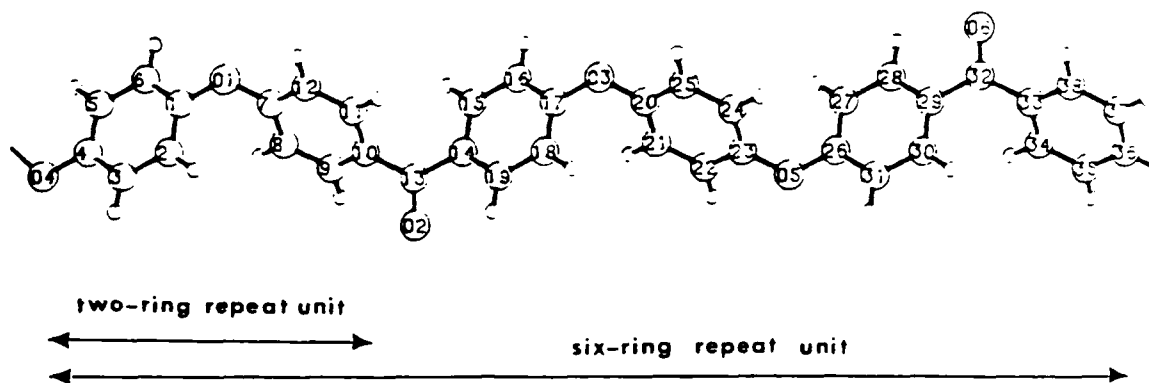


Figure 1 Atom numbering scheme of carbon atoms for the two- and six-ring repeat units. Hydrogen atoms are numbered according to the carbon atoms to which they are attached

cameras employing Ni-filtered $\text{CuK}\alpha$ radiation. A bundle of 3 monofilaments furnished sufficient sample mass to provide reasonable exposure times. Photographs were recorded with various exposure times in order to bring all reflections into the correct range of optical density.

The diffraction patterns were indexed in terms of an orthorhombic unit cell. Accurate unit cell dimensions were obtained by a least-squares refinement of the d -spacings of 15 diffraction peaks on precession photographs.

Intensity measurements

Fibre rotation photographs were scanned on an Optronics Photoscan P1000 microdensitometer. The instrument records the optical density (OD) at each point on the film as a binary integer on magnetic tape. The digitized patterns were then processed by the computer program PHOTO⁸. The peak volume option gave a number representing the integrated intensity of each peak. A background correction was made for each peak by averaging the OD at the four corners of a box enclosing the peak. The peak volume versus exposure time plot was found to be linear to approximately $OD = 1.5$. However, to ensure that the measurements corresponded to the linear portion of the plot, only peak volume measurements on peaks with $OD = 1.0$ or less were used. Reflections which could not be resolved were treated as an overlapping group. Lorentz and polarization corrections were applied directly to the peak volume data. Structure factors were derived from $F_{\text{obs}} = (I/LP)^{1/2}$.

RESULTS

X-ray analysis and density measurement

The fibre rotation and precession photographs are shown in Figure 2. The unit cell parameters $a = 7.83 \pm 0.02 \text{ \AA}$, $b = 5.94 \pm 0.01 \text{ \AA}$ and $c = 9.86 \pm 0.04 \text{ \AA}$ are in good agreement with previously reported values^{2,3}. They refer to the subcell, which contains the two-ring unit of Figure 1. The dimensions deduced for the complete Pbcn unit cell are identical to those of the subcell, except that the c dimension is tripled (29.58 \AA). The c -axis is 1 \AA less than the value (30.50 \AA) reported by Wakelyn for various powder specimens³.

The crystal density based on the subcell dimensions and an average molecular weight of 192.2 daltons is 1.392 g cm^{-3} . The calculated crystal density based on the

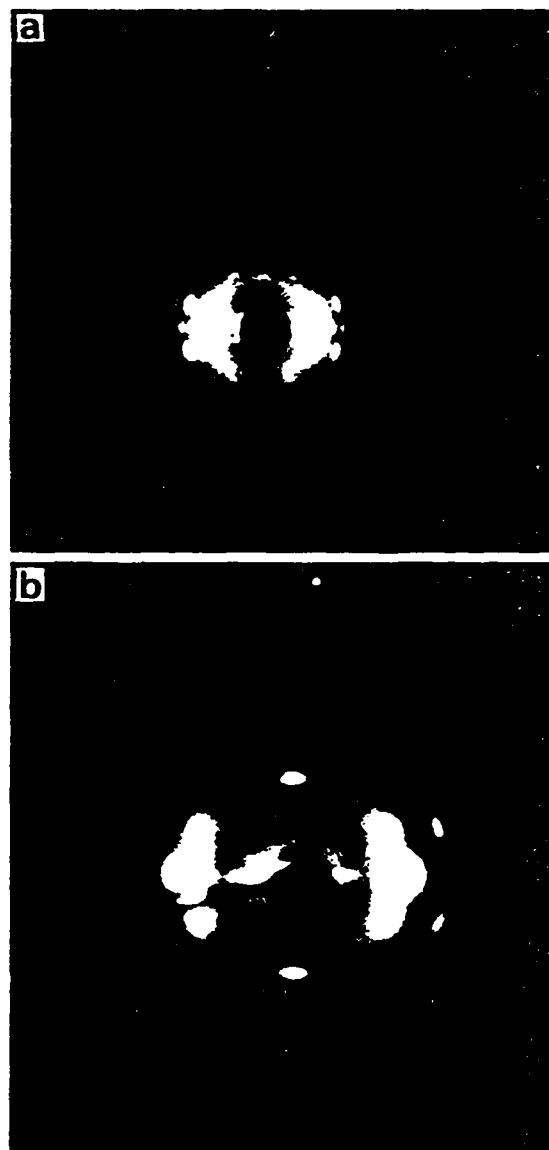
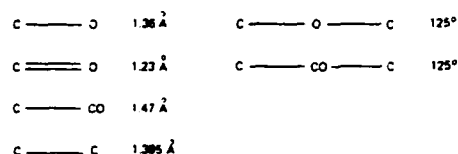


Figure 2 (a) Fibre rotation photograph, $\text{CuK}\alpha$ radiation, camera radius 28.6 mm; (b) precession photograph, zero layer screen, $\mu = 25^\circ$, $\text{CuK}\alpha$ radiation, sample to film distance 6.0 cm. The fibre direction is vertical in both photographs

unit cell parameters of Rueda *et al.*² is 1.415 g cm^{-3} , and 1.400 g cm^{-3} for the cell of Dawson and Blundell¹. The monofilament fibre density measured $1.298 \pm 0.005 \text{ g cm}^{-3}$ by the flotation method and $1.296 \pm 0.005 \text{ g cm}^{-3}$ by the buoyancy method. Experimental densities are reported to vary from 1.264 g cm^{-3} for quenched amorphous specimens to 1.314 g cm^{-3} for oriented samples^{1,2}. A linear extrapolation has yielded 1.378 g cm^{-3} for the crystal density³.

Refinement of the two-ring unit

The small quantity of diffraction data (20 observed peaks) coupled with the rather large number of chain conformational torsion angles precluded the refinement of the six-ring unit (Figure 1). The strategy adopted to obtain the initial orientation of the phenylene rings involved the refinement of the two-ring unit, positioned within the unit subcell described above. Two phenylene rings connected by alternating ether and carbonyl links comprise the two-ring unit. The ratio of the respective site-occupancy factors (s.o.f.) for these linkage groups was held fixed at either 1:1 or 2:1. The latter ratio served to represent a disordered chain in which the composition of the crystallographic repeat matched the known chemical repeat of the polymer. The initial trial model for the LALS method was constructed using the following literature values for bond distances and angles:^{3,9}



Two chains, related by a 2/1 screw axis and aligned along the *c*-axis, were placed in the subcell with the centre of the phenylene ring of one chain at the origin. Refinement was effected by varying the chain conformation angles t_1 - t_5 and the orientation of the chain within the subcell. Angles t_3 and t_5 were constrained so that their initial difference was always zero degrees in order to maintain 2-fold rotational symmetry along the carbonyl bond. Refinement was terminated when the *R*-index,

$$R = \frac{\sum |F_o - F_c|}{\sum |F_o|}$$

did not change on successive cycles. The results are summarized in Table 1. The function minimized in the least-squares procedure contained terms which represented the deviations of the calculated interatomic distances from the desired values. The coincidence constraints between pairs of atoms related by

Table 1 Results of the refinement of the two-ring unit

Torsion angle	<i>t</i> (degrees)	
	S.o.f. ratio (ether:ketone)	
	1:1	2:1
t_1 C ⁻ -O1-C1-C2	45.3	44.3
t_2 CS-C ⁻ -O1-C1	37.5	43.9
t_3 O2-C13-C10-C9	-38.6	-37.7
t_4 C14-C13-C10-C9	138.6	132.5
t_5 C15-C14-C13-C10	-38.6	-37.7
<i>R</i> -index (%)	27.0	24.6

translational symmetry along *c* were also included. Throughout the refinement the isotropic temperature factor remained fixed at $B = 6.0 \text{ \AA}^2$. The angle t is defined as follows: If the section of chain C2-C1-O1-C7 is viewed from C7 down the O1-C1 bond, then t_1 is positive if clockwise rotation of the front bond (C7-O1) brings it into eclipsed configuration with the back bond (C1-C2).

The refinement of the disordered chain gave the expected improvement in the *R*-index; however, the average of the magnitudes of t_1 , t_2 and t_3 changed only slightly. The shortest intermolecular contact for the 1:1 calculation was 2.52 \AA between atoms O2 and H8 on chains related by the 2/1 screw axis. The contacts for the disordered calculation were normal, except for one very short contact (1.64 \AA) involving the disordered carbonyl oxygen atom. With standard deviations as large as 3° for t , the differences between the magnitudes of t_1 , t_2 and t_3 were hardly significant at this level of refinement. For the 1:1 calculation the average tilt of the phenylene rings out of the (100) face was 40° . Hay *et al.*³ arrived at the same value for crystalline PEEK by employing a procedure adopted by Rietveld of fitting the wide-angle diffraction pattern¹⁰. The sum of the magnitudes of t_3 and t_4 for the 1:1 calculation approaches 180° , which strongly suggested that the ring carbon atoms attached to the ketone and ether oxygen atoms do not deviate significantly from the (100) face. Such deviations would still be consistent with Pbcn symmetry. A similar conclusion may be drawn for the 2:1 calculation even though the sum of t_3 and t_4 of 170° makes the argument less convincing. Thus the planar zig-zag geometry of C-O-C and C-OC-C links is restricted to the (100) face. This arrangement is now carried over to the refinement of the six-ring unit.

Conformation of the six-ring unit

Based on the results of the two-ring refinement a single torsion angle t was used to describe the conformation of the six-ring unit (Figure 1). The initial placement of the chains followed the description of Wakelyn⁵. The *R*-index was computed for a range of fixed t values. The variables which remained to be refined were the angles defining the inclination of the molecule within the unit cell, and a scale

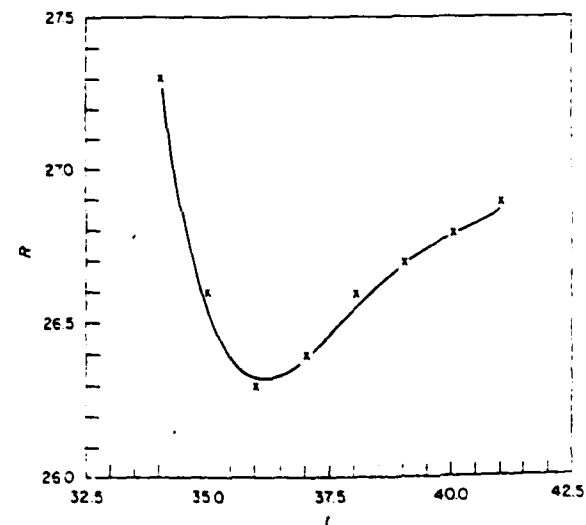
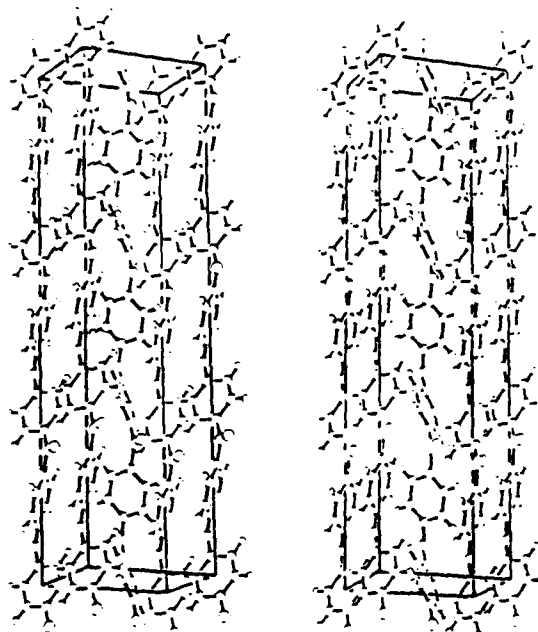


Figure 3 Plot of *R*-index versus *t*

Figure 4 Stereodiagram of unit cell viewed down the negative *b*-axisTable 2 Observed and calculated *d*-spacings and structure amplitudes ($\times 10$)

<i>h</i>	<i>k</i>	<i>l</i>	d_o (Å)	d_c (Å)	F_o	F_c	
1	1	0	4.75	4.72	2707	2153	
1	1	3	4.29	4.26	1430	1042	
1	0	6	4.17	4.17	583	483	
2	0	0	3.96	3.93	2248	2528	
1	1	6	3.42	3.41	496	356	
2	1	3	3.09	3.10	1075	563	
0	2	0	2.98	2.98	912	557	
1	1	9	2.73	2.72	434	352	
2	1	6	2.72	2.72	633	592	
1	2	3	2.66	2.67	542	659	
3	1	0	2.39	2.39	482	430	
2	2	0	2.36	2.36			
3	1	3	2.31	2.32	866	913	
2	2	3		2.30			
2	1	9	-	2.32	231	357	
3	0	6	-	2.31	201	450	
1	1	12	-	2.18	971	601	
1	3	0	-	1.92	799	668	
0	2	12	-	1.90	949	800	
1	3	3	-	1.88			
1	3	2	3	-	1.92	1051	634
1	3	6	-	1.79	245	27	
1	2	12	-	1.70	556	417	
1	3	1	12	-	1.72		

* d_o values were measured from precession photographs

factor. Even though space group symmetry requires the carbonyl function to coincide with the 2-fold rotation axis at (0, $\frac{1}{4}$), the restriction was relaxed and the molecule was allowed to rotate freely about the *c*-axis. As measured by the difference of the *x* coordinates of atoms C13 and O2, no significant deviation (approximately 0.1 Å) of the carbonyl bond from the rotation axis was observed. The smallest deviations were observed when *t* was in the range 37°–40°. The variation of the *R*-index with *t* is illustrated in Figure 3. The minimum is fairly broad and *t* of 37° was considered the best fit based on the minimum in the *R*-

index and the extent of deviation of the carbonyl bond from the 2-fold axis. The uncertainty in *t* was estimated to be about 3°. A stereodiagram of the unit cell is shown in Figure 4. Observed and calculated *d*-spacings and

Table 3 Fractional atomic coordinates of the six-ring unit for the case where $t = 37^\circ$

Atom	<i>x</i>	<i>y</i>	<i>z</i>
O1	0.021	-0.212	0.082
O2	-0.042	0.426	0.251
O3	0.021	-0.212	0.419
O4	-0.021	0.212	-0.082
O5	-0.021	0.212	0.584
O6	0.042	-0.426	0.752
C1	0.011	-0.107	0.042
C2	0.053	0.104	0.036
C3	0.072	0.211	-0.006
C4	-0.011	0.107	-0.042
C5	-0.083	-0.104	-0.036
C6	-0.072	-0.211	0.006
C7	0.011	-0.107	0.123
C8	-0.100	0.073	0.129
C9	-0.111	0.180	0.171
C10	-0.011	0.107	0.207
C11	0.100	-0.073	0.201
C12	0.111	-0.180	0.159
C13	-0.022	0.220	0.251
C14	-0.011	0.107	0.295
C15	-0.083	-0.104	0.301
C16	-0.072	-0.211	0.342
C17	0.011	-0.107	0.378
C18	0.083	0.140	0.372
C19	0.072	0.211	0.331
C20	0.011	-0.107	0.460
C21	-0.100	0.073	0.465
C22	-0.111	0.180	0.507
C23	-0.011	0.107	0.543
C24	0.100	-0.073	0.537
C25	0.111	-0.180	0.495
C26	-0.011	0.107	0.624
C27	-0.083	-0.104	0.630
C28	-0.072	-0.211	0.672
C29	0.011	-0.107	0.708
C30	0.083	0.104	0.702
C31	0.072	0.211	0.660
C32	0.022	-0.220	0.752
C33	0.011	-0.107	0.796
C34	-0.100	0.073	0.802
C35	-0.111	0.180	0.843
C36	-0.011	0.107	0.879
C37	0.100	-0.073	0.873
C38	0.111	-0.180	0.832
H2	0.143	0.180	0.062
H3	0.125	0.364	-0.010
H5	-0.143	-0.180	-0.062
H6	-0.125	-0.364	0.010
H8	-0.173	0.126	0.103
H9	-0.191	0.310	0.175
H11	0.173	-0.126	0.226
H12	0.191	-0.310	0.155
H15	-0.143	-0.180	0.275
H16	-0.125	-0.364	0.346
H18	0.143	0.180	0.398
H19	0.125	0.364	0.326
H21	-0.173	0.126	0.440
H22	-0.191	0.310	0.511
H24	0.173	-0.126	0.563
H25	0.191	-0.310	0.491
H27	-0.143	-0.180	0.604
H28	-0.125	-0.364	0.676
H30	0.143	0.180	0.728
H31	0.125	0.364	0.656
H34	-0.173	0.126	0.776
H35	-0.191	0.310	0.848
H37	0.173	-0.126	0.899
H38	0.191	-0.310	0.828

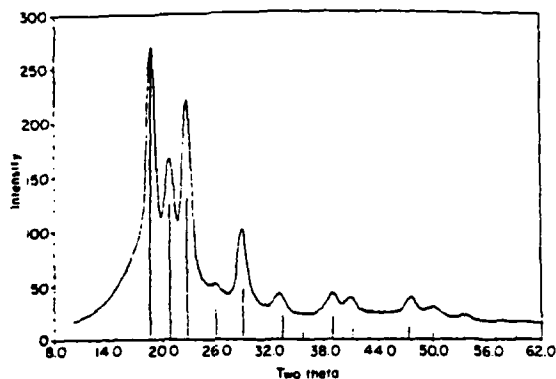


Figure 5 Comparison of the simulated powder pattern (peaks displayed as vertical lines) with the X-ray diffractogram of an unoriented PEEK specimen. The simulated powder pattern was calculated using the POWD7 program and the coordinates of the six-ring unit in Table 3

structure factors for the case of $t = 37^\circ$ are compared in Table 2, and the corresponding atomic fractional coordinates are presented in Table 3. With the suspicion that the space group was not Pbcn, another symmetry operation relating the two-chains was tried: namely, a 2-fold rotation axis replaced the 2₁ screw axis. The resulting intermolecular contacts were unsatisfactory and the *R*-index was considerably higher.

Simulated powder pattern

The computer program POWD7¹¹ was utilized to calculate the theoretical powder diffractogram of PEEK. The calculation assumes Laue symmetry mmm and is based on the coordinates of the six-ring unit of Table 3. The half-width of a diffraction profile was taken to be 1.0° at $2\theta = 20^\circ$. The theoretical peak positions (displayed as vertical lines) are compared in Figure 5 with the experimental X-ray diffractogram of an unoriented specimen prepared by melt-quenching (400°C) a sample of PEEK resin. The four major calculated peaks (18.76° , 20.82° , 22.72° and 28.78°) are indexed 110, 113, 200 and 213, respectively. Weaker peaks (with indices) are also found at 32.88° (216), 33.52° (123) and 38.78° (313). The

results are in good agreement with published X-ray diffractograms for various PEEK samples³.

CONCLUSIONS

The structure of crystalline PEEK fibre has been analysed using accurate diffraction intensities from fibre rotation patterns. The analysis supports and extends to monofilaments the previously reported finding for other PEEK specimens that space group Pbcn is a valid representation of the structure. Atomic coordinates are derived for the six-aryl ring unit and are used as input parameters in the calculation of a theoretical powder pattern. A comparison of the experimental and theoretical patterns provides additional support for the Pbcn space group assignment.

ACKNOWLEDGEMENTS

We thank Dr J. Cantrell for performing density measurements and C. George for technical assistance. The fibre studied was kindly provided by M. Storrier of Albany International. We are indebted to Dr D. P. Anderson, University of Dayton Research Institute, for providing the diffraction diagram of unoriented PEEK. One of us (A.V.F.) gratefully acknowledges a research contract by the Monsanto Research Corporation.

REFERENCES

- 1 Dawson, P. C. and Blundell, D. J. *Polymer* 1980, 21, 577
- 2 Rueda, D. R., Ania, F., Richardson, A., Ward, I. M. and Balta Calleja, F. J. *Polymer* 1983, 24 (Commun.), 258
- 3 Hay, J. N., Kemmish, D. J., Langford, J. I. and Rae, A. I. M. *Polymer* 1984, 25 (Commun.), 175
- 4 Yoda, O. *Polymer* 1985, 26 (Commun.), 16
- 5 Wakelyn, N. T. *Polymer* 1984, 25 (Commun.), 306
- 6 Boon, J. and Magre, E. P. *Makromol. Chem.* 1969, 126, 130
- 7 Smith, P. J. C. and Arnott, S. *Acta Cryst.* 1978, A34, 3
- 8 Anderson, D. P. Documentation of 'Photo': A User's Manual for the Analysis of Photographic and X-ray Negatives. Air Force Tech. Report AFWAL-TR-84-4159, Feb., 1985
- 9 Pattabhi, V. and Venkatesan, K. J. *Cryst. Mol. Struct.* 1973, 3, 25
- 10 Rietveld, H. M. *Acta Cryst.* 1967, 22, 151; *J. Appl. Cryst.* 1969, 2, 65
- 11 Smith, D. K. and Holomany, M. 'POWD7: A Fortran Program for Calculating Powder Diffraction Patterns'. Dept. of Geosciences, Pennsylvania State University, 1980

J. MACROMOL. SCI.—PHYS., B24(1-4), 159-179 (1985-1986)

The Structure of Poly-2, 5-benzoxazole (ABPBO) and Poly-2,6-benzothiazole (ABPBT) Fibers by X-Ray Diffraction*

ALBERT V. FRATINI[†] and ELISA M. CROSS
Department of Chemistry
University of Dayton
Dayton, Ohio 45469

JOSEPH F. O'BRIEN and W. WADE ADAMS
Materials Laboratory
Air Force Wright Aeronautical Laboratories
Wright-Patterson Air Force Base, Ohio 45433

Abstract

The determination of the crystalline structure of oriented fibers of poly-2,5-benzoxazole (ABPBO) and poly-2,6-benzothiazole (ABPBT) is described. Both unit cells are metrically orthorhombic, with the parameters: $a = 6.061$ (17), $b = 3.384$ (13), c (fiber axis) = 11.575 (6) Å for ABPBO; and $a = 6.044$ (6), $b = 3.417$ (7), c (fiber axis) = 12.194 (18) Å for ABPBT. The fiber repeat consists in each structure of two fused ring groups arranged in a planar, zigzag conformation. The conformational torsion angle and orientation of chains within the unit cells are derived from

*Presented at the Symposium on Polymer Diffraction, Philadelphia, Pennsylvania, August 26, 1984

[†] To whom correspondence should be addressed.

a linked-atom least squares refinement technique. Polymer chains pack laterally through van der Waals interactions. A plausible disorder model which involves defects in chain direction is presented. Refinement of a static disorder model for ABPBO in which 50% of the chains have their chain directions reversed leads to a lower R residual and sum of constraints.

INTRODUCTION

Success in achieving exceptional mechanical properties and high temperature stability in fibers produced from extended chain polymers such as poly(p-phenylene terephthalamide) (PPTA) has encouraged investigations of other stiff-chain and rigid-rod polymers. The Materials Laboratory, through its Air Force Ordered Polymer Research Program [1], has sought to take advantage of the thermal and oxidative stability of the aromatic heterocyclic class of polymers, and to explore their engineering properties.

Recently, this effort has focused on the stiff-chain ABPBX (X = S, O, N) molecular structures. Two of the polymers synthesized as part of this program are illustrated in Figs. 1 and 2: poly-2,5-benzoxazole (ABPBO) and poly-2,6-benzothiazole (ABPBT). They show improved thermal stability over the poly-

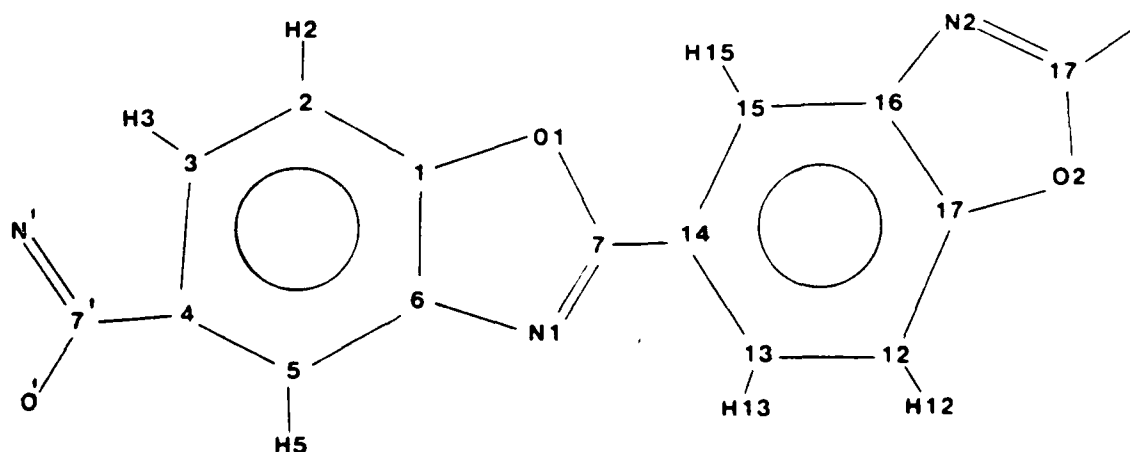


FIG. 1. The chemical structure of poly-2,5-benzoxazole (ABPBO) showing the atom numbering scheme. The three primed atoms N^1 , 7^1 , and O^1 were constrained to coincide with atoms N_2 , 17, and O_2 , establishing chain continuity in the linked-atom least squares refinement.

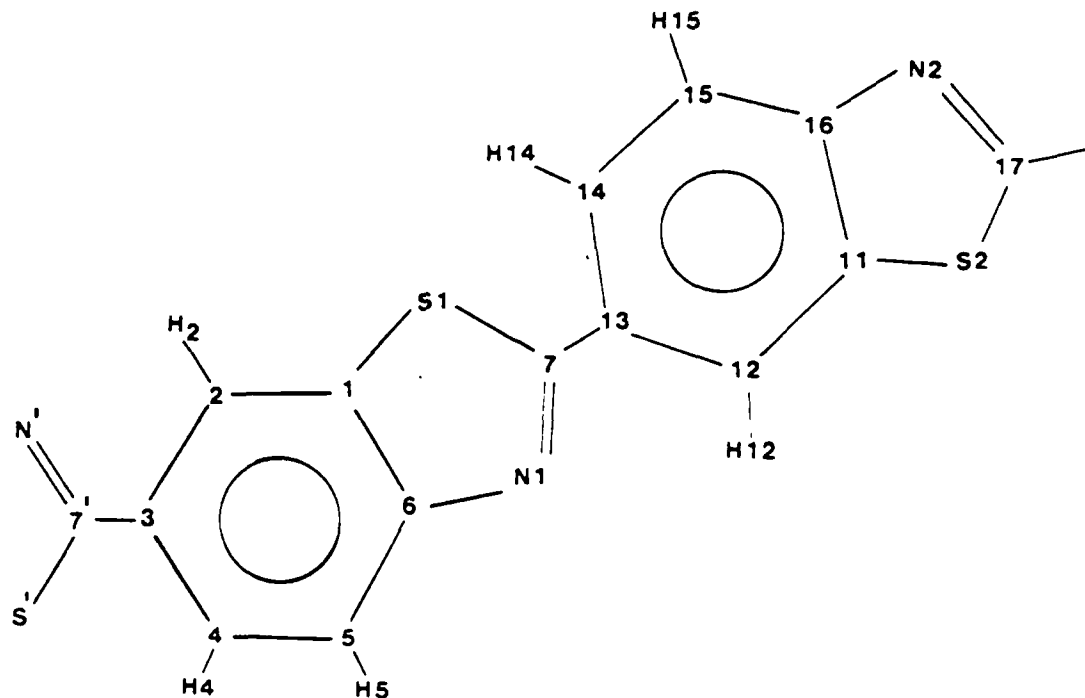


FIG. 2. The chemical structure of poly-2,6-benzothiazole (ABPBT) showing the atom numbering scheme. The three primed atoms N^1 , 7^1 , and S^1 were constrained to coincide with atoms N2, 17, and S2, establishing chain continuity in the linked-atom least squares refinement.

amides and poly(p-phenylene benzobisthiazoles), and do not have the moisture sensitivity of the benzimidazole structures. Because of their semiflexible nature, both polymers form lyotropic, nematic phases in which the chains are presumably well aligned but are not in axial registry [2]. Spinning fibers from a liquid crystalline phase has distinct advantages. Besides enhancing the flow properties of the system, the polymer chains already have much of the ordering required in the crystalline fibrous state to exhibit the desired superior mechanical properties. This paper reports the crystalline structures of these two polymers.

EXPERIMENTAL METHODS

Materials

Oriented fibers of ABPBO and ABPBT were spun at elevated temperatures from liquid crystalline dopes containing polyphosphoric acid. Fibers were spun by W-F. Hwang of the Univer-

sity of Dayton Research Institute and M. Hunsaker of the AFWAL Materials Laboratory. Dopes were supplied by J. F. Wolfe of SRI International [3]. Monofilaments were heat treated under constant strain in a nitrogen atmosphere.

Recording of X-Ray Diffraction Data

Diffraction intensities were collected using a conventional Weissenberg camera employing Ni-filtered $\text{CuK}\alpha$ radiation. The entire range of intensities was recorded by the multiple-film method. Fiber rotation patterns are shown in Fig. 3. The fiber axis is perpendicular to the x-ray beam, and coaxial with the film.

Diffraction patterns were also recorded on a Buerger precession camera and are shown in Fig. 4. These photographs simplified the indexing of diffraction spots, in addition to providing accurate d-spacings for use in the determination of unit cell parameters. Integrated intensities were also measured from precession patterns. None of the intensities, however, was used in the structure refinement due to the uncertainty in the appropriate Lorentz factor of the meridional reflections [4].

Determination of Unit Cell Parameters

The diffraction patterns for ABPBO and ABPBT were indexed in terms of orthogonal (metrically orthorhombic) unit cells. The unit cell parameters (see Table 1) were refined by minimizing the sum of the squares of the differences between observed and calculated d-spacings. Measured fiber densities were obtained by the flotation method.

Determination of Integrated Intensity of Diffraction Maxima

Fiber rotation patterns were scanned with an Optronics Photoscan P1000 microdensitometer. The PHOTO computer program [5] displayed the digitized pattern as iso-optical density contours on the screen of a graphics terminal. The "peak volume" option gave the volume of each spot, after correcting for background intensity. Because some spots were too weak to appear as a contour on the screen, their peak volumes were visually estimated. A calibration plot showed the optical density (OD) to be linear with exposure time to $\text{OD} = 1.4$. However, to ensure that the measurements corresponded to a linear portion

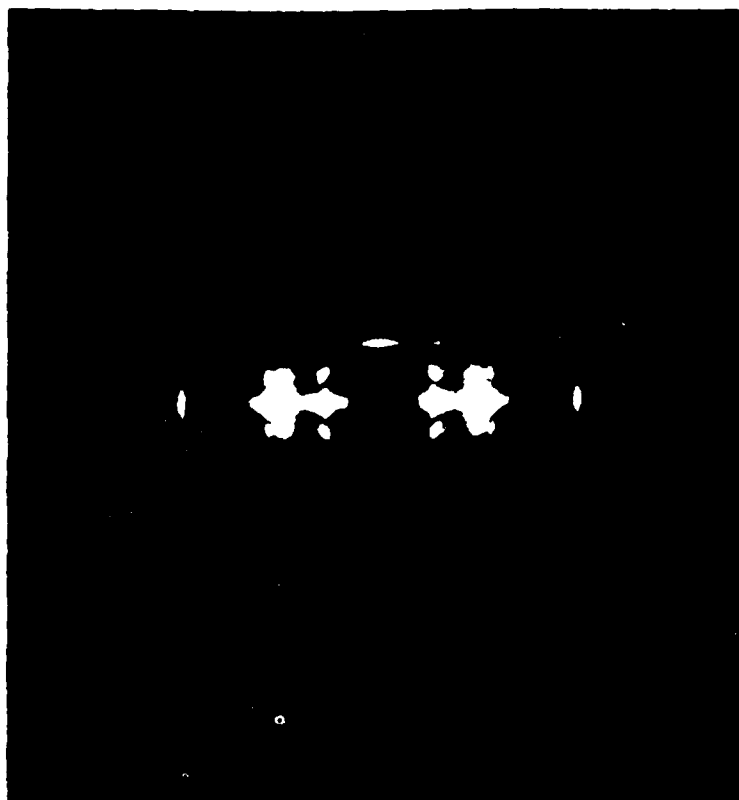
TABLE 1
Diffraction Data for ABPBO and ABPBT

	ABPBO	ABPBT
a (Å)	6.061 (17)	6.044 (6)
b (Å)	3.384 (13)	3.417 (7)
c (Å)	11.575 (6)	12.194 (18)
Unit Cell Symmetry	Orthogonal (pseudo-orthorhombic)	Orthogonal (pseudo-orthorhombic)
Chain symmetry	2_1	2_1
Molecules per cell (Z)	1	1
Formula unit	$[C_{14}H_6N_2O_2]_n$	$[C_{14}H_6N_2S_2]_n$
Formula units per fiber repeat (n)	2	2
Calculated density ($g\ cm^{-3}$)	1.638	1.756
Measured density ($g\ cm^{-3}$)	1.4	1.5

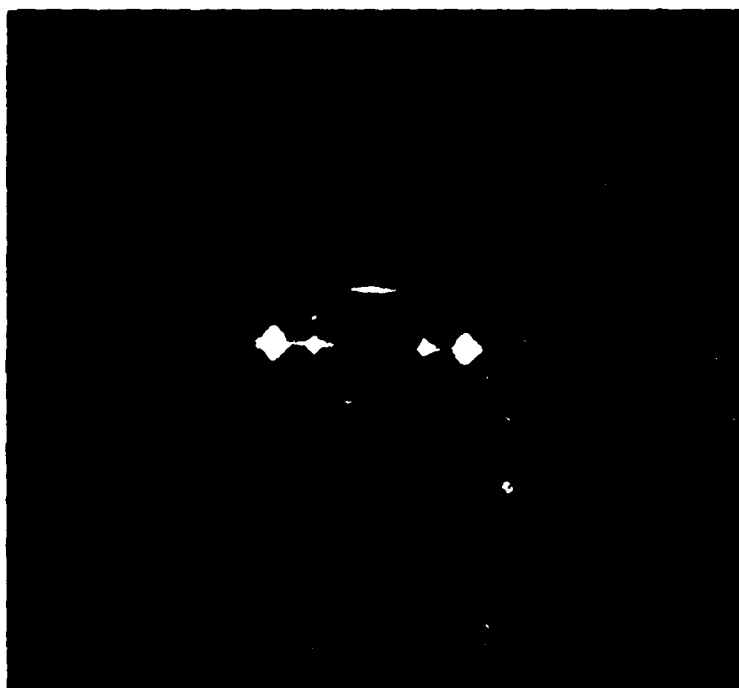
of the plot, only peak volume measurements on peaks with OD ≤ 1.0 were used. Because of the observed linearity, the peak volume was taken to be directly proportional to the integrated intensity of the diffraction spot. The intensity was apportioned between partly overlapping reflections. Reflections which could not be resolved were treated as an overlapping group. Finally, Lorentz and polarization corrections were applied directly to the peak volume data resulting in observed structure factors, F_o .

Determination of Chain Conformation and Refinement

Planar zigzag chain structures in which two fused ring groups comprise the crystallographic (fiber) repeat were chosen for the initial models on the basis of the observed fiber periods. In support of this model were the systematic absences $00l$, $l = 2n + 1$, indicative of a 2_1 screw axis along the chain



(a)



(b)

FIG. 3. Fiber rotation photograph (fiber direction vertical) of ABPBO (a) and ABPBT (b): $\text{CuK}\alpha$ radiation, camera radius 28.6 mm.

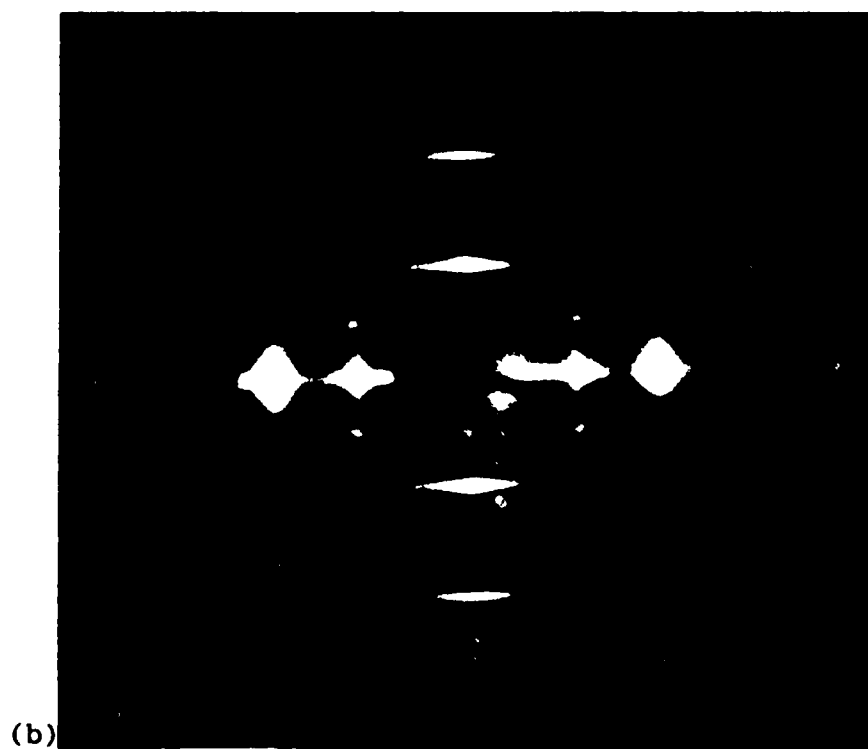


FIG. 4. Buerger precession patterns of ABPBO (a) and ABPBT (b): fiber direction vertical, zero layer screen, $\mu = 25^\circ$, $\text{CuK}\alpha$ radiation, sample-to-film distance 6.0 cm.

TABLE 2
Selected Fixed Bond Lengths and
Bond Angles Incorporated in
Starting Models

ABPBO		ABPBT	
Lengths (Å)			
C7-C14	1.467	C7-C13	1.468
C7-N1	1.300	C7-N1	1.300
C7-O1	1.370	C7-S1	1.762
Angles (°)			
N1-C7-O1	115.6	N1-C7-S1	115.5
N1-C7-C14	127.3	N1-C7-C13	124.0

axis. Values for bond lengths and angles (Table 2) were assumed to be the same as those found in comparable model compounds [6-8]. Thus, only the one conformational torsion angle (τ) between planes of the ring groups plus the three orientation parameters of the molecules within the unit cell were refined for each structure.

The linked-atom least squares (LALS) technique for the refinement of polymer structures has been described by Smith and Arnott [9]. The function minimized was

$$\theta = \sum_i w_i \Delta F_i^2 + \sum_j k_j \Delta D_j^2 + \sum_k \lambda_k G_k$$

where ΔF_i is the difference between observed and calculated values of the i th structure factor, and w_i (taken to be unity) is the assigned weight. ΔD_j is the deviation of the calculated interatomic distance from the desired minimum value, and k_j is a weight. The third term imposes the coincidence constraints between pairs of atoms related by translational symmetry along the c axis in order to ensure chain continuity. A scale factor K was also included as a variable in the refinement, and a constant overall isotropic temperature factor B of 6.0 \AA^2 was used. Refinement was terminated when the crystallographic reliability index, $R = \Sigma |\Delta F| / \Sigma F_0$, did not change on successive cycles.

RESULTS

Parameters defining the chain conformation and orientation within the unit cell together with the R factor (calculated with observed reflections only) are given in Table 3. The orientation angles X, Y, and Z refer to the rotation angle about the x, y, and z axes, respectively, required to bring the chain into its correct orientation. Positive rotation is clockwise when viewed from positive infinity along each axis. The initial placement of the chain in the unit cell is accomplished by placing the root atom (C14 for ABPBO and C13 for ABPBT) on the c axis with the bond to its precursor (C7 in each structure) pointing along the positive x axis and its precursor (N1 for each structure) in turn lying in the (x,-y) plane.

The molecular conformation and packing within the unit cell are illustrated in Figs. 5-10 with space-filling drawings. The van der Waals radii are scaled down from their normal values in order to allow easier visualization of the structure. Fractional atomic coordinates are presented in Tables 4 and 5. Calculated and observed d-spacings and structure factors are listed in Tables 6 and 7.

TABLE 3
Parameters Defining Chain Conformation and
Chain Orientation within Unit Cell

	ABPBO	ABPBT
Torsion angle (τ) ($^{\circ}$)	0.0	0.0
X ($^{\circ}$)	90.0	90.0
Y ($^{\circ}$)	-120.4	-82.5
Z ($^{\circ}$)	5.3	4.0
R factor (%)	20.8	9.5
	(based on 14 Bragg maxima)	(based on 10 Bragg maxima)

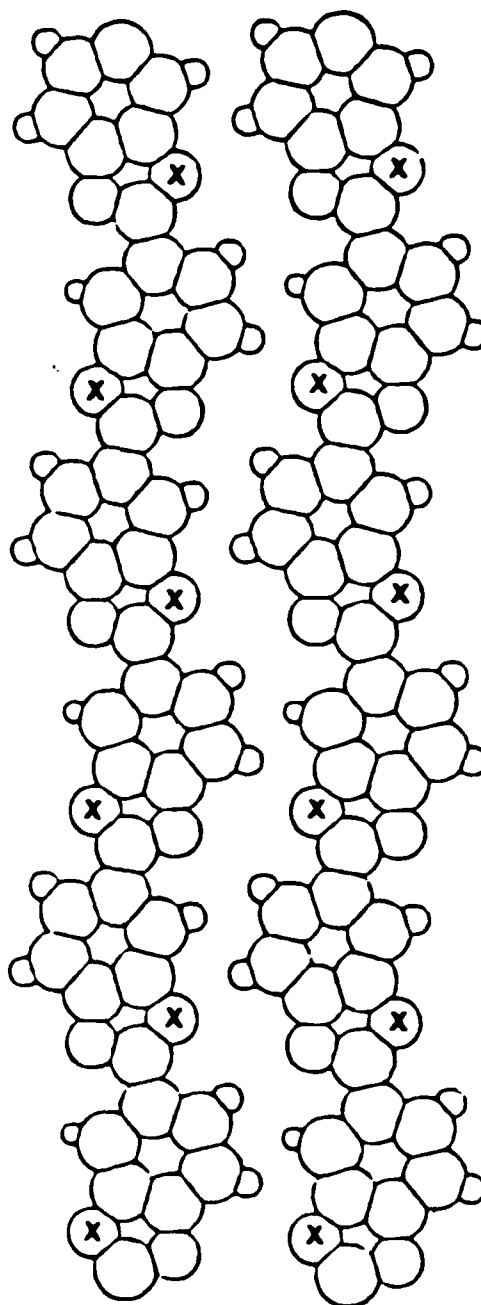


FIG. 5. Ring normal view of two chains of ABPBO separated by one translation along the a axis. x denotes the nitrogen atom.

TABLE 4
Fractional Atomic Coordinates for ABPBO

Atom	X	Y	Z
H2	-0.579	0.096	0.228
C2	-0.422	0.070	0.202
C3	-0.373	0.062	0.085
H3	-0.494	0.082	0.027
C4	-0.158	0.026	0.047
C5	0.013	-0.002	0.127
H5	0.169	-0.028	0.099
C6	-0.046	0.008	0.242
N1	0.087	-0.014	0.341
C7	-0.052	0.009	0.426
O1	-0.269	0.045	0.396
C1	-0.267	0.044	0.277
C14	0.000	0.000	0.550
C13	0.216	-0.036	0.586
H13	0.337	-0.056	0.528
C12	0.268	-0.045	0.703
H12	0.426	-0.071	0.728
C11	0.095	-0.016	0.778
O2	0.104	-0.017	0.897
C17	-0.112	0.019	0.931
N2	-0.255	0.042	0.847
C16	-0.128	0.021	0.747
C15	-0.194	0.032	0.632
H15	-0.353	0.059	0.613

TABLE 5
Fractional Atomic Coordinates for ABPBT

Atom	X	Y	Z
H2	-0.209	0.026	0.097
C2	-0.064	0.008	0.125
C3	0.114	-0.014	0.050
C4	0.330	-0.040	0.087
H4	0.445	-0.054	0.035
C5	0.377	-0.046	0.198
H5	0.523	-0.064	0.224
C6	0.202	-0.025	0.270
N1	0.223	-0.027	0.383
C7	0.031	-0.004	0.431
S1	-0.198	0.024	0.342
C1	-0.017	0.002	0.231
C13	0.000	0.000	0.550
C12	0.179	-0.022	0.624
H12	0.324	-0.040	0.596
C11	0.130	-0.016	0.735
S2	0.310	-0.038	0.846
C17	0.081	-0.010	0.935
N2	-0.111	0.014	0.887
C16	-0.090	0.011	0.774
C15	-0.265	0.032	0.702
H15	-0.411	0.050	0.727
C14	-0.218	0.027	0.591
H14	-0.333	0.041	0.539

STRUCTURE OF ABPBO AND ABPBT FIBERS

171

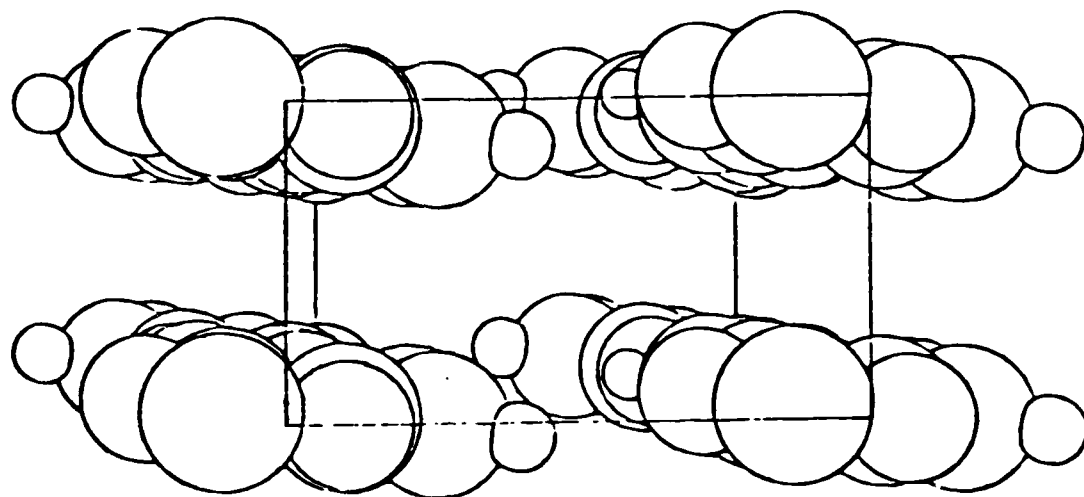


FIG. 6. c axis (fiber axis) view of unit cell of ABPBO. The a axis is horizontal.

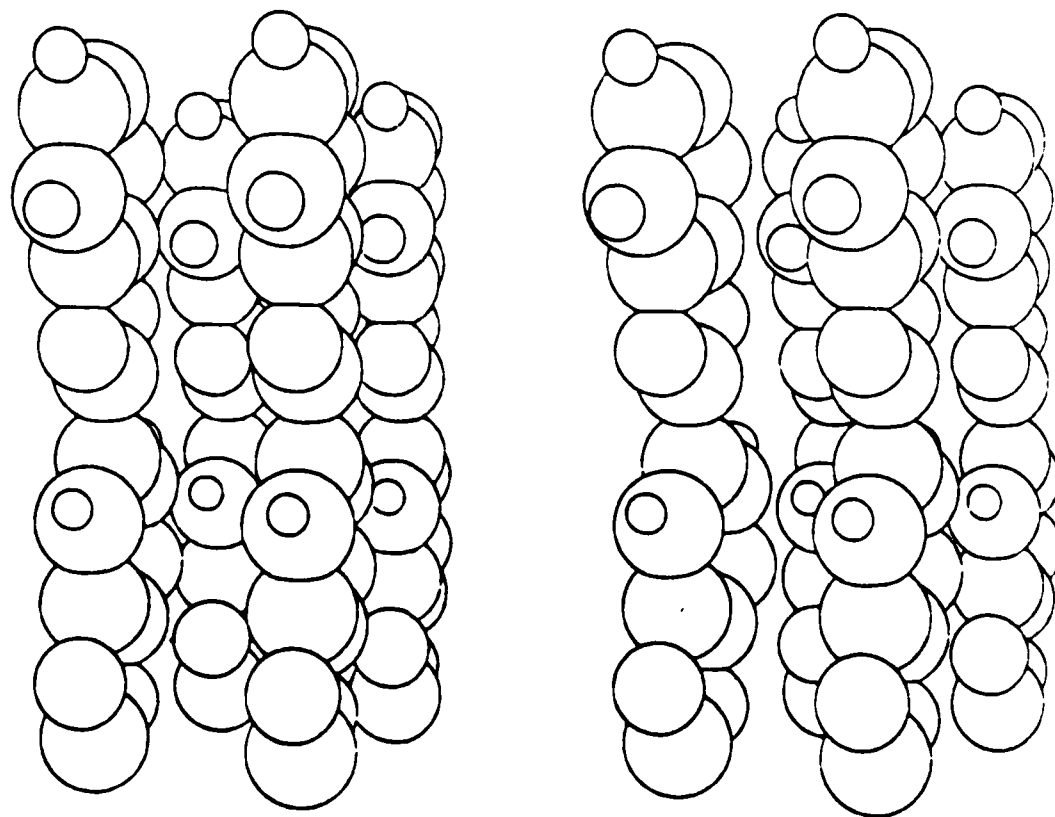


FIG. 7. Stereoview along the a axis of unit cell of ABPBO.

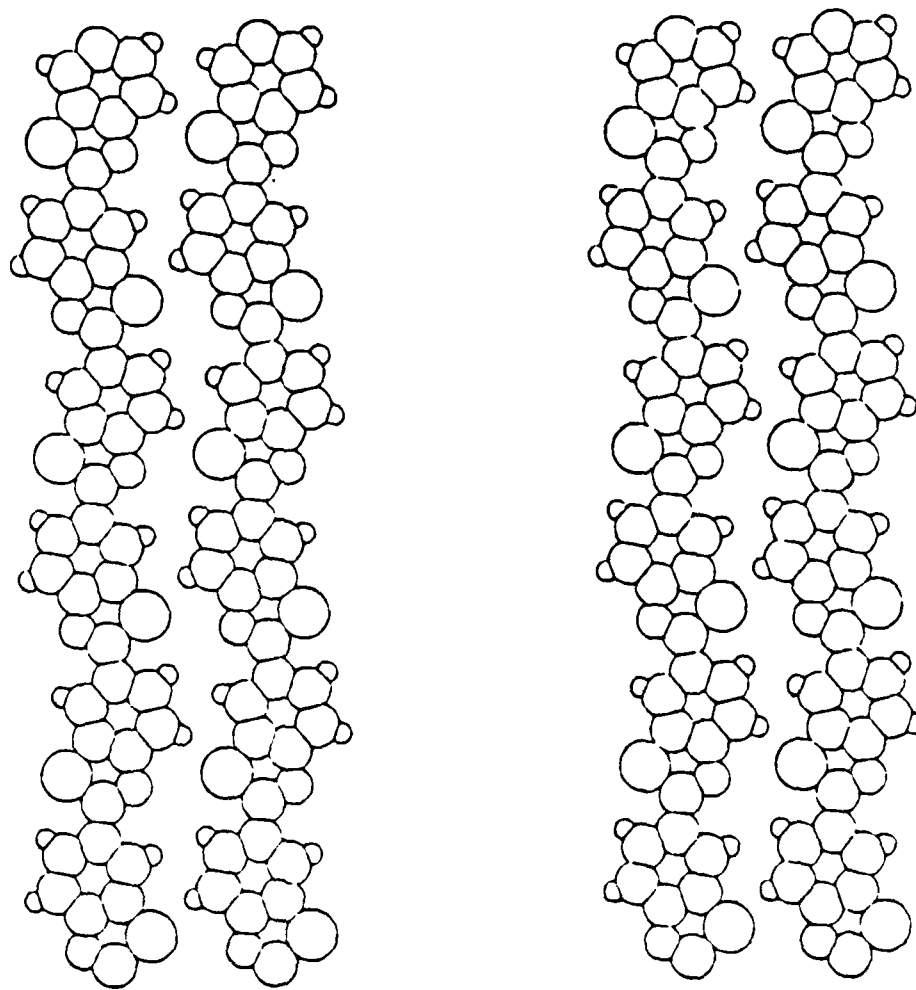


FIG. 8. Ring normal stereoview of two chains of ABPBT separated by one translation along the a axis. The largest sphere signifies the sulfur atom.

STRUCTURE OF ABPBO AND ABPBT FIBERS

173

TABLE 6
Observed and Calculated Spacings and
Structure Amplitudes ($\times 10$)
for ABPBO

h k l	d_o (Å) ^a	d_c (Å)	F_o	F_c
1 0 1	5.36	5.37	116	154
1 0 0	6.08	6.06	375	417
1 1 0 } 0 1 0 }	3.38	2.95 } 3.38 }	897	860
1 1 1 } 2 0 1 }	2.93	2.86 } 2.93 }	126	176
1 0 3	3.29	3.25	33	48
1 1 4 } 0 1 4 } 2 0 4 }	2.15	2.07 } 2.20 } 2.09 }	81	139
1 0 2	4.20	4.19	71	108
0 2 0	—	1.69	271	253
3 0 1	—	1.99	50	76
3 0 2	—	1.91	78	122
3 0 4	—	1.66	102	82
1 2 0	—	1.63	173	234
1 1 3 } 2 0 3 }	—	2.35 } 2.38 }	41	88
1 1 2 } 2 0 2 }	—	2.63 } 2.68 }	16	90

^aAccurate d_o values could not be measured for the more diffuse reflections.

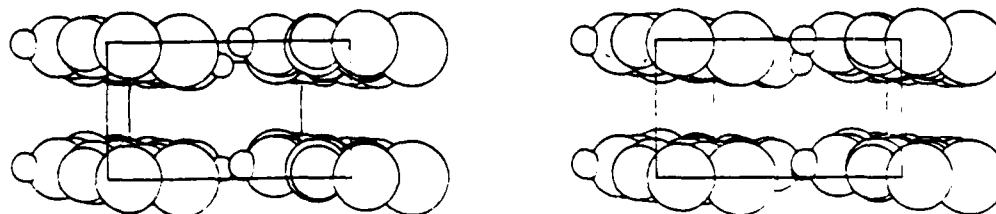


FIG. 9. Stereoview along the c axis (fiber axis) of unit cell of ABPBT. The a axis is horizontal.

TABLE 7
Observed and Calculated Spacings and
Structure Amplitudes ($\times 10$)
for ABPBT

$h\ k\ \ell$	d_o (Å)	d_c (Å)	F_o	F_c
1 0 1	5.39	5.42	111	165
1 0 0	6.06	6.04	379	388
0 1 0	3.42	3.42	868	878
2 0 2	2.71	2.71	152	178
2 0 0	3.03	3.02	271	213
2 0 4	2.15	2.15	226	230
1 2 0	1.65	1.64	211	198
0 2 0	1.75	1.71	398	355
2 0 1	2.93	2.93	68	112
1 0 3	—	3.37	144	135

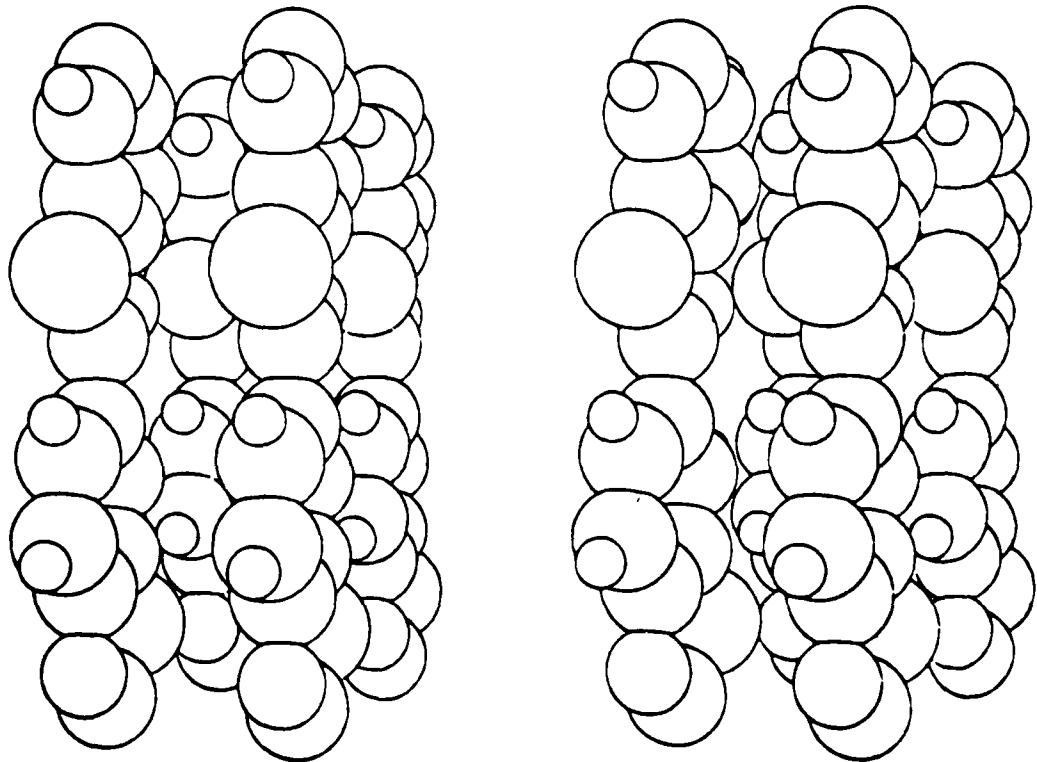


FIG. 10. Stereoview along the a axis of unit cell of ABPBT.

DISCUSSION

The presence of a number of hkl Bragg maxima in the x-ray patterns of Figs. 3 and 4 is taken as evidence for three-dimensional order in fibers of ABPBO and ABPBT. It thus becomes possible for each polymer to solve the structure by conventional x-ray methods.

As is shown in Table 1, the lattice dimensions of the two unit cells are very similar, except for the fiber identity period. Although the unit cells are observed to be metrically orthorhombic, the polymer chains lack the requisite Laue symmetry for the assignment of a primitive, orthorhombic space group. An orthogonal, monoclinic space group possessing a 2_1 screw axis would probably be a reasonable choice. The lack of knowledge of a unique space group did not thwart the attempt at a structure analysis in a primitive unit cell.

The packing arrangements of the planar zigzag chains are also quite similar (Figs. 5-10). A layered or sheet structure of planar molecules is not strictly observed since the molecular planes are tilted out of the (100) face by 5.3° for ABPBO and 4.0° for ABPBT. The perpendicular separation between planes is roughly the same as the b-axis length, 3.4 Å. Inspection of Table 8 shows that overly short intra- and interchain atomic distances are not found. The shortest interchain distance for ABPBO is 2.02 Å for H2 . . . H15, and the shortest value in ABPBT is 2.21 Å for H12 . . . H14.

CNDO/2 molecular orbital calculations recently reported by Welsh and Mark [10] corroborate the observed coplanar arrangement of atoms in ABPBO. Conformational energy minima are observed at $\tau = 0^\circ$ and 180° , the $\tau = 0^\circ$ conformation being slightly preferred by about 0.1-0.20 kcal/mol. The barrier to free rotation about the single rotatable bond was found to be about 1.6 kcal/mol, so that rotation is facile at heat treatment temperatures of over 300°C . Thus the observed enhancement in molecular ordering following heat treatment under tension presumably is associated with this type of motion.

The structures reported in this paper are somewhat idealized since the assumed primitive lattice requires the chains to be in perfect registry, as would be the case in a highly crystalline material. The diffuseness of diffraction maxima, especially along the meridian, and the streaking visible along the $hk1$ and $hk2$ layer lines are clear indications of some axial translational disorder. A similar situation, but to a much greater extent, has been observed for the chemically related, rigid-rod poly(p-phe-

TABLE 8
Intra- and Interchain Atomic Distances (Å)^a

ABPBO		ABPBT	
H2 .. H15(I)	2.02	H12 .. H14(I)	2.21
H13 .. H15(I)	2.20	S2 .. H15(I)	2.24
H5 .. H2(I)	2.24	H4 .. H2(I)	2.24
H5 .. H3(I)	2.31	H5 .. S1(I)	2.24
O2 .. H5(II)	2.38	H5 .. H2(I)	2.26
H12 .. N2(I)	2.45	H12 .. H15(I)	2.28
N1 .. H2(I)	2.51	S2 .. H4(II)	2.45
N2 .. H3(II)	2.52	C17 .. H4(II)	2.52
C17 .. H3(II)	2.55	N2 .. H2(II)	2.63
H15 .. O1(III)	2.56		
C12 .. H15(I)	2.60		
C17 .. H5(II)	2.62		
H12 .. C15(I)	2.63		
H13 .. N1(III)	2.65		

^aThe left-hand member of each pair of atoms has parameters (xyz) corresponding to those listed in Tables 4 and 5. The parameters for the atom on the right are indicated as follows: (I) $x + 1, y, z$; (II) $x, y, z + 1$; (III) x, y, z .

nylene benzobisthiazoles (PBT) [11-13]. The molecular origin of this disorder can be understood, on one hand, by allowing the axial slippage of well-aligned chains past each other. For molecules stacked directly above one another (i.e., along the direction perpendicular to the molecular planes), the predictions of the minimum energy arrangement are that the chains are out of register by 1.5 Å for PBT and by as large as 3.0 Å in the case of poly(p-phenylene benzobisoxazole) (PBO) [14].

It should be noted that the polymer chain has directionality; that is, it has a distinct up and down sense, and is not centrosymmetric. Thus an energetically feasible packing arrangement might be possible by mixing chains with opposite senses. Figure 11 illustrates a packing arrangement which includes a single defect chain. A 180° rotation of the defect chain about the chain axis does not introduce still another disorder mode since translation of the defect chain by half the fiber repeat returns it to the position shown in Fig. 11. If chain reversal were to occur on a large scale, then one would expect that the packing order of the fiber would be decreased. However, sev-

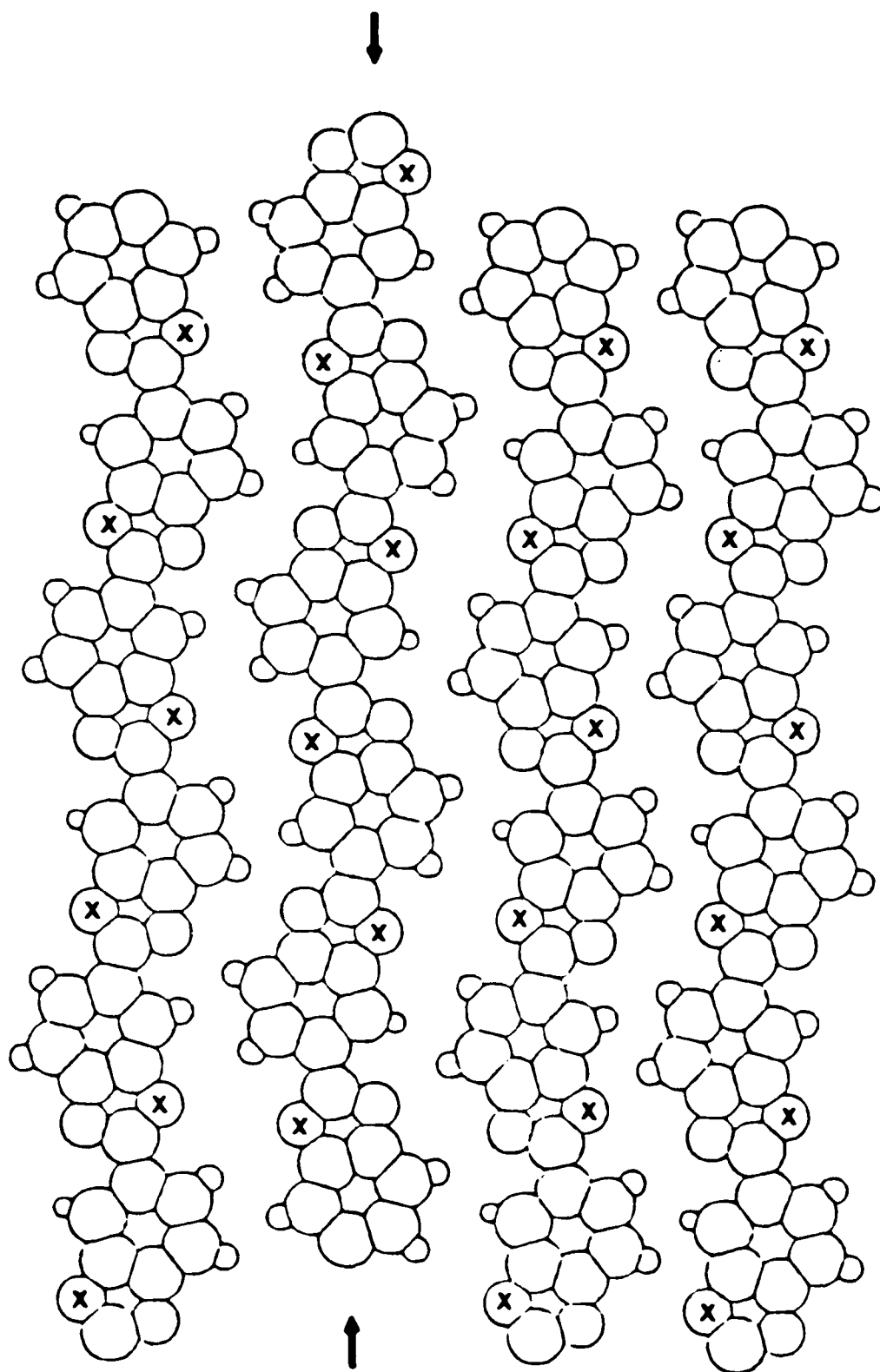


FIG. 11. Representation of a possible disorder mode in ABPBO viewed normal to molecular planes. The arrow denotes the chain in the opposite direction. x indicates the nitrogen atom.

eral polymers with irregular sequences such as atactic poly(vinyl alcohol) and poly(methylene) polysulfides are highly crystalline [15], so caution must be exercised in concluding that chain directionality is regular in ABPBO and ABPBT.

In order to ascertain the effect of chain reversal on the structure of ABPBO, LALS refinement was carried out on a unit cell in which 50% of the chains have their senses reversed. Chains were positioned in the lattice such that adjacent chains ran in opposite directions. Reversed chains were translated by one-half the c-axis length in order to preserve the zigzag packing arrangement. Several cycles of refinement yielded a three percent lower R index with a slight reduction in the sum of constraints. The conformational torsional angle remained about 0° . A lower value for the residual is to be expected since refinement of this disorder model introduces additional parameters corresponding to the angular rotation about the c axis of each of four chains. Nevertheless, this type of disorder is considered reasonable based on the fact that there are no new short intermolecular contacts.

The structures presented here should aid in the understanding of the relationship between molecular order, morphology, and properties of these polymers. The high degree of order, which is comparable to that observed for PPTA, is undoubtedly associated with the high tensile modulus of these fibers. We plan further work to examine chain directional defects in non-primitive unit cells.

Acknowledgment

One of us (A.V.F.) gratefully acknowledges the support of the Air Force Office of Scientific Research through grant AFOSR-84-0364.

REFERENCES

- [1] T. E. Helminiak, Preprints of ACS Division of Organic Coatings and Plastics Chemistry, 40, 475 (1979).
- [2] P. J. Flory, Proc. Roy. Soc. London, A 234, 60 (1956).
- [3] J. F. Wolfe and P. D. Sybert, private communication, U. S. Patent application No. W084/01162.
- [4] R. D. B. Fraser, T. P. Macrae, A. Miller and R. J. Rowlands, J. Appl. Cryst., 9, 81 (1976).
- [5] D. P. Anderson, Documentation of "PHOTO": A User's Manual for the Analysis of Photographic and X-ray negatives, Air Force Tech. Report AFWAL-TR-84-4159, Feb. 1985.

STRUCTURE OF ABPBO AND ABPBT FIBERS

179

- [6] M. W. Wellman, W. W. Adams, R. A. Wolff, D. R. Wiff and A. V. Fratini, *Macromolecules*, 14, 935 (1981).
- [7] M. W. Wellman, W. W. Adams, D. R. Wiff and A. V. Fratini, *Air Force Tech. Report AFML-TR-79-4184*, Part I.
- [8] P. Groth, *Acta Chem. Scand.*, 27, 945 (1973).
- [9] P. J. Campbell Smith and S. Arnott, *Acta Cryst.* A34, 3 (1978).
- [10] W. J. Welsh and J. E. Mark, *Polym. Eng. Sci.*, accepted for publication.
- [11] W. W. Adams, L. V. Azároff and A. K. Kulshreshtha, *Z. Kristallogr.* 150, 321 (1979).
- [12] E. J. Roche, T. Takahashi and E. L. Thomas, *Fiber Diffraction Methods*, A.C.S. Symp. Ser., No. 141, 303 (1980).
- [13] J. A. Odell, A. Keller, E. D. T. Atkins and M. J. Miles, *J. Mat. Sci.*, 16, 3309 (1981).
- [14] D. Bhaumik, W. J. Welsh, H. H. Jaffé and J. E. Mark, *Macromolecules*, 14, 951 (1981).
- [15] K. Suehiro, Y. Chatani and H. Tadokoro, *Polymer Journal*, 7, 352 (1975).

Accepted by Editor March 26, 1985

STRUCTURE OF POLYBENZOBISOXAZOLE AND POLYBENZOBISTHIAZOLE FIBERS

A. V. Fratini, Department of Chemistry, University of Dayton,
Dayton, Ohio 45469, and W.W. Adams, Materials Laboratory,
AFWAL/MLBP, Wright-Patterson Air Force Base, Ohio 45433.

The structure of as-spun fibers of poly(p-phenylene benzobisoxazole) (PBO) and poly(p-phenylene benzobisthiazole) (PBT) has been viewed as arrays of molecules organized laterally on a two-dimensional lattice, with translational disorder along the chain axis. Heat treatment improves the extent of three-dimensional order and the axial tensile modulus of these rigid rod polymers. In particular, a correlation is expected between the degree of three-dimensional order and the compressive modulus, and is the subject of the present study. Diffraction patterns of heat treated PBO fibers exhibiting several hkl diffraction maxima have been interpreted in terms of a primitive, monoclinic unit cell with dimensions $a = 5.64(3)$, $b = 3.58(1)$, $c = 12.07(1)$ Å, and $\gamma = 100.4(3)^\circ$. The structure was refined using a linked-atom least-squares procedure employing intensities obtained from fiber rotation photographs. The primitive cell contains very short nonbonded contacts between hydrogen atoms of the bisoxazole moieties. A similar situation exists for PBT. Refinement of a larger two-chain unit cell will be presented. Such a cell allows for slippage parallel to the chain axis and a variable azimuthal orientation of one chain relative to the other.

STRUCTURE OF AROMATIC HETEROCYCLIC RIGID ROD AND STIFF CHAIN
POLYMERS

J. F. O'Brien and W. W. Adams, Materials Laboratory,
Wright-Patterson Air Force Base, Ohio 45433.

A. V. Fratini and E. Cross, Department of Chemistry, University of
Dayton, Dayton, Ohio 45469.

X-ray diffraction methods were used to investigate the lateral packing in rod-like poly(p-phenylene benzobisthiazole), (PBT), poly(p-phenylene benzobisoxazole), (PBO), and stiff chain poly(2,5(6)benzoxazole), (ABPBO), and poly(2,6-benzothiazole), (ABPBT). The current model for the 3-d crystalline polymers ABPBO and ABPBT contains a fiber repeat with two monomer units in the fully extended, planar zig-zag conformation, in an orthogonal lattice of dimensions $\underline{a} = 6.06(2)$, $\underline{b} = 3.38(1)$, $\underline{c} = 11.575(6)$ Å for ABPBO, while for ABPBT the dimensions are $\underline{a} = 6.04(1)$, $\underline{b} = 3.42(1)$, and $\underline{c} = 12.19(2)$ Å. The fiber structure of PBT and PBO, which was viewed as 2-d laterally ordered arrays of molecules with translational disorder along the chain axis, now has more 3-d character, as shown by x-ray diffractometer scans along the layer lines compared to calculated molecular transforms.

Model Compounds For Aromatic Heterocyclic Polymers. The X-Ray Crystal Structures of 1,4-Bis(2-benzoxazolyl)-2,5-bis(2-benzimidazolyl)benzene and 2,6-Bis[2-(2-benzothiazolyl)phenyl]benzo[1,2-d:4,5-d']bisthiazole

by

Albert V. Fratini, Margaret A. Sturtevant, Jacque D. Henes

University of Dayton, Dayton, Ohio 45469

and

W. Wade Adams

Materials Laboratory, Wright Aeronautical Laboratories

Wright-Patterson Air Force Base, Ohio 45433

INTRODUCTION

The Polymer Synthesis Groups located in the Polymer Branch of the Materials Laboratory, Wright-Patterson Air Force Base, have synthesized a series of model compounds which are capable of providing structural data for the class of aromatic heterocyclic polymers. Figure 1 shows the chemical structures of four of these model compounds. Of particular interest are those compounds which are applicable to the structure determination of the rigid rod PBX polymers containing bulky benzothiazole, benzoxazole and benzimidazole substituents. It has been shown in the case of PBT that the presence of pendant groups along the polymer backbone results in improved solubility and compressive strength properties. The work described below involves the application of x-ray crystallographic methods to the determination of the structures of compounds (2) and (4).

1,4-Bis(2-benzoxazolyl)-2,5-bis(2-benzimidazolyl)benzene (4)

Experimental

A pale yellow needle of $C_{34}H_{20}N_6O_2$ having dimensions 0.20 x 0.20 x 0.40 mm was mounted with its needle axis nearly coincident with the ϕ -axis of an Enraf-Nonius CAD4/Micro-11 diffractometer, equipped with MoK_{α} radiation and graphite monochromator. Cell constants and an orientation matrix for data collection were obtained from least-squares refinement of the setting angles of 25 reflections in the range $6^{\circ} < \theta < 16^{\circ}$. The space group, triclinic cell parameters and calculated volume are: $P\bar{1}$, $a = 6.035(1)$, $b = 8.623(2)$,

$a = 12.512(3) \text{ \AA}$, $\alpha = 74.39(2)^\circ$, $\beta = 79.43(2)^\circ$, $\gamma = 87.99(2)^\circ$, and $V = 616.4 \text{ \AA}^3$. Assuming $Z=1$ and a formula weight of 544.6, the calculated crystal density is 1.47 g cm^{-3} . The measured density as determined by flotation in a dichloromethane/carbon tetrachloride mixture is 1.472 g cm^{-3} .

The data were collected at 295K using the $\omega/2\theta$ scan mode, ω width $(0.8 + 0.34 \tan \theta)^\circ$. A variable scan rate was employed which permits rapid data collection for intense reflections when a fast scan rate is used and assures good counting statistics for weak reflections when a slow scan rate is used. Data were collected to a maximum 2θ of 60° . Moving-crystal moving-counter background counts were made by scanning an additional 25% above and below this range. The counter aperture was adjusted as a function of θ . The vertical aperture was set at 4.0 mm. For strong reflections an attenuator was automatically inserted in front of the detector; the attenuator factor was 17.5.

Data Reduction

A total of 3152 unique reflections were collected. As a check on crystal and electronic stability three representative reflections were measured every 120 minutes. A linear decay correction of 0.1% was applied. Lorentz and polarization corrections were applied; no absorption corrections were made ($\mu = 0.90 \text{ cm}^{-1}$ for $\text{MoK}\alpha$ radiation).

Structure Solution and Refinement

All calculations were performed on a VAX/730 computer using the Enraf-Nonius Structure Determination Package SDP/VAX v3.0. The structure was solved by direct methods. Hydrogen atoms were located in difference Fourier maps. The structure was refined by full-matrix least-squares where the

function minimized was $\sum w(|F_o| - |F_c|)^2$ and weight w is defined as $4F_o^2/\sigma^2(F_o^2)$. A total of 1886 reflections having intensities greater than 3.0 times their standard deviation were used in the refinement. The final cycle of refinement included 217 variable parameters and converged with unweighted and weighted agreement factors of $R = 0.063$ and $R_w = 0.063$. The highest peak in the final difference map had a height of $0.37 \text{ e}/\text{Å}^3$. Plots of $\sum w(|F_o| - |F_c|)^2$ versus $|F_o|$, reflection order in data collection, $\sin(\theta/\lambda)$, and various classes of indices showed no unusual trends.

Discussion

The structure of the molecule is shown in Figure 2. Tables 1 and 2 contain the fractional atomic coordinates and anisotropic thermal parameters for the non-hydrogen atoms. The bond lengths and angles of the non-hydrogen atoms are given in Tables 3 and 4. Selected torsion angles are presented in Table 5.

The molecule is positioned on a crystallographic center of inversion and is therefore centrosymmetric. All ring systems are planar. The least-squares plane of the benzoxazole moiety is rotated by 5° from coplanarity with the central benzene ring; the corresponding value for the benzimidazole group is 57° . Potentially short contacts involving the benzimidazole hydrogen atom would preclude a more coplanar arrangement between the central benzene ring and the benzimidazole substituents. The benzimidazole group is disordered as evidenced by the difficulty in accurately positioning the benzimidazole hydrogen atom and the near equality of distances N2-C14 and N3-C14.

2,6-Bis[2-(2-benzothiazolyl)phenyl]benzo[1,2-d:4,5-d']bisthiazole (2)

Except where noted below, the experimental and data collection conditions as well as the methods of data reduction, structure solution and refinement used for (2) were similar to those previously discussed for (4).

Experimental and Data Conditions

A yellow irregularly shaped crystal of $C_{34}H_{18}N_8S_4$ of dimensions 0.50 x 0.25 x 0.35 mm was mounted in a random orientation on the diffractometer. Cell constants and an orientation matrix for data collection were obtained from the least-squares refinement of the setting angles of 25 reflections in the range $3^\circ < \theta < 14^\circ$. The monoclinic cell parameters and calculated volume are $a = 16.377(2)$, $b = 16.332(2)$, $c = 12.251(3)$ Å, $\beta = 121.53(1)^\circ$, and $V = 2792.8$ Å³. For $Z=4$ and a formula weight of 610.8, the calculated density is 1.45 g cm⁻³. The measured density obtained by flotation in a cyclohexane/carbon tetrachloride mixture is 1.46 g cm⁻³. The systematic absences (hkl , $h+k$ odd and $h0l$, l odd) are compatible with space groups Cc and $C2/c$. The correct space group was later confirmed to be $C2/c$. The data were collected at 295K to a maximum $2\theta=60^\circ$.

Data Reduction

A total of 8024 reflections were collected, of which 3931 were unique. A linear decay correction was applied; the correction factor on I ranged from 1.000 to 1.013 with an average value of 1.006. The linear absorption coefficient is 3.6 cm⁻¹ for MoK radiation. Absorption corrections were not applied. Intensities of equivalent reflections were averaged. The agreement

factors for the averaging of 1629 observed and accepted reflections were 3.5% based on intensity and 3.3% based on F_o .

Structure Solution and Refinement

The structure was solved by direct methods. 730 reflections having intensities greater than 3.0 times their standard deviation were used in the refinement. The final cycle of refinement converged with R of 0.046 and R_w of 0.057. The highest peak in the final difference map had a height of 0.22 e/Å³.

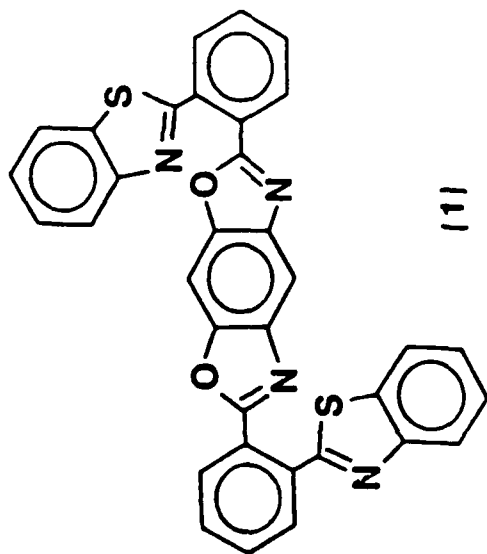
Discussion

Tables 6 and 7 contain positional and thermal parameters for the non-hydrogen atoms. Bond lengths, angles and selected torsion angles are given in Tables 8, 9 and 10. Two labelled PLUTO drawings showing different views of the molecule are presented in Figures 3 and 4.

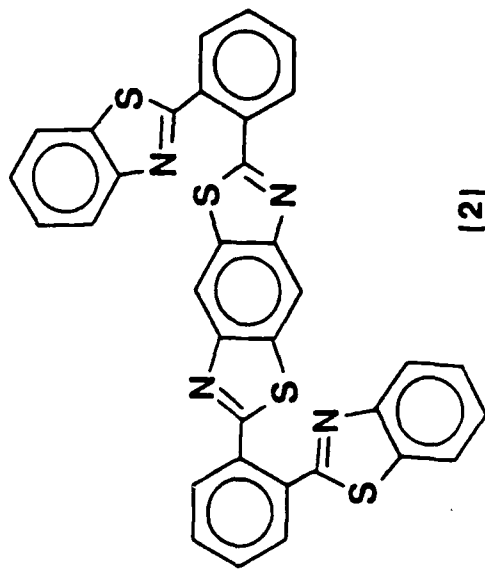
The molecule is centrosymmetric. The twist angle between the 2-benzothiazolylphenyl substituent and the benzobisthiazole segment is 56°. The benzothiazole ring system is rotated by 56° from coplanarity with the attached phenyl ring. Sulfur atoms S1 and S2 have a cis arrangement.

FIG. 1

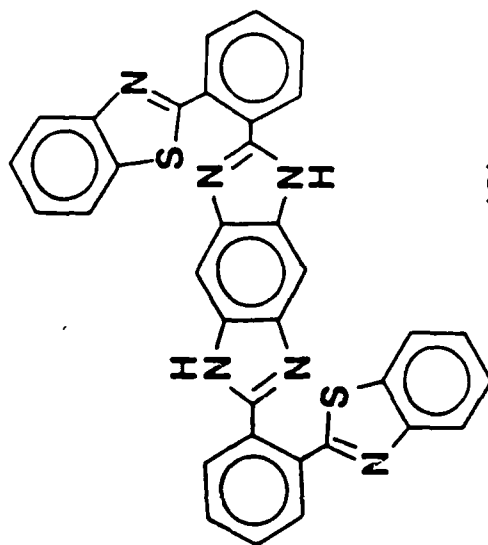
MODEL COMPOUNDS



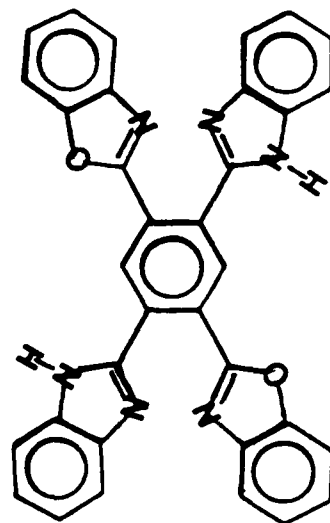
(11)



(12)



(13)



(14)

Preprint 1

Fig. 2

Preprint 1

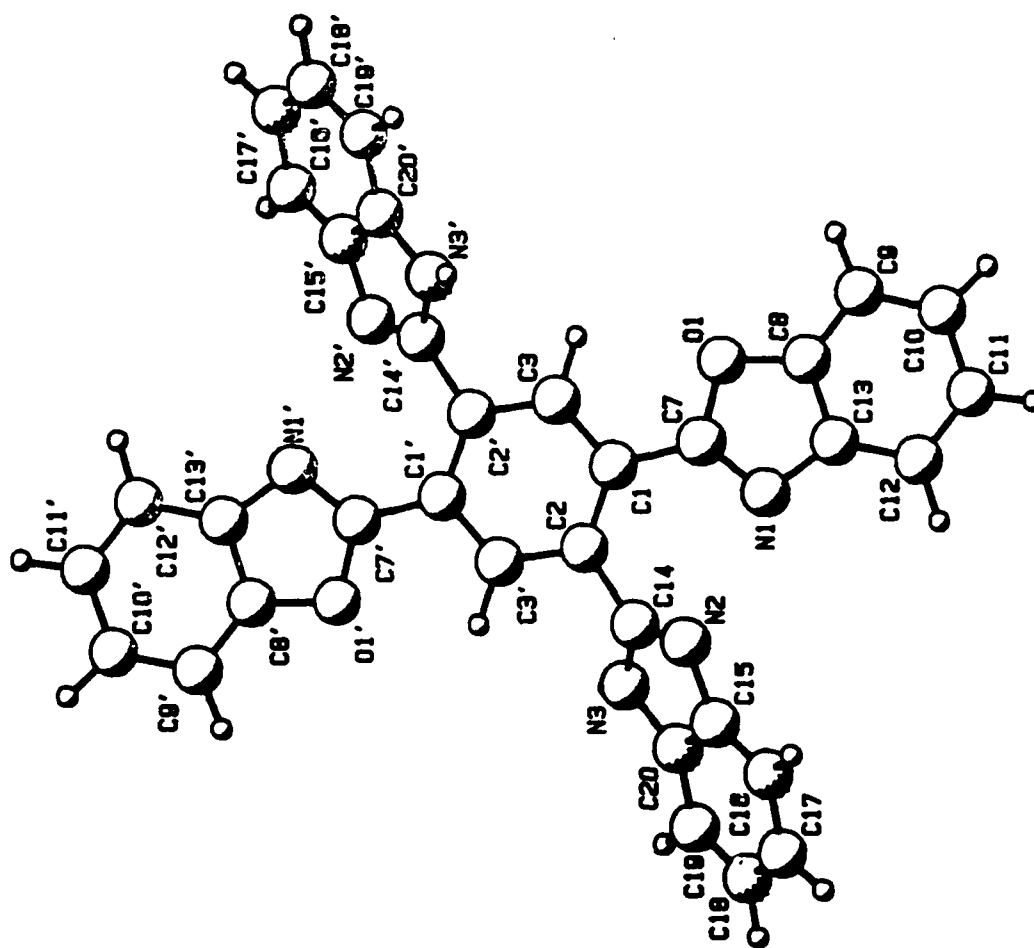


Fig. 3

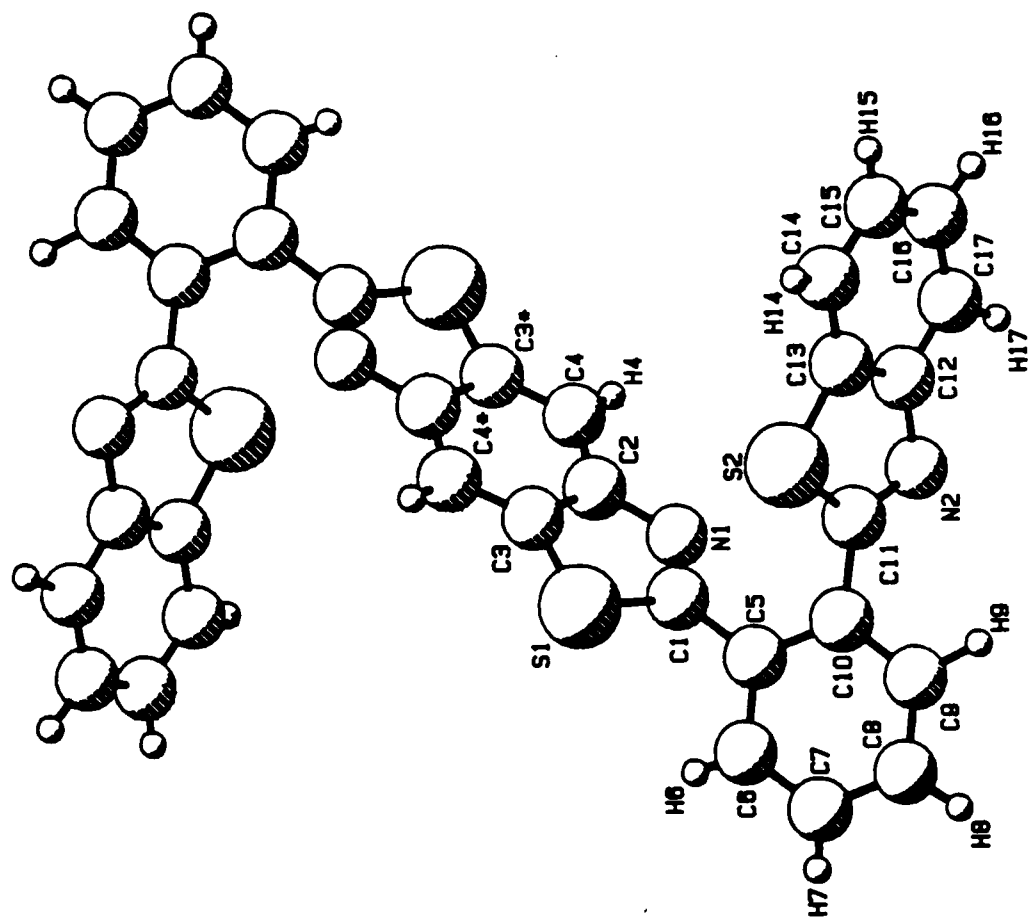


Fig. 4

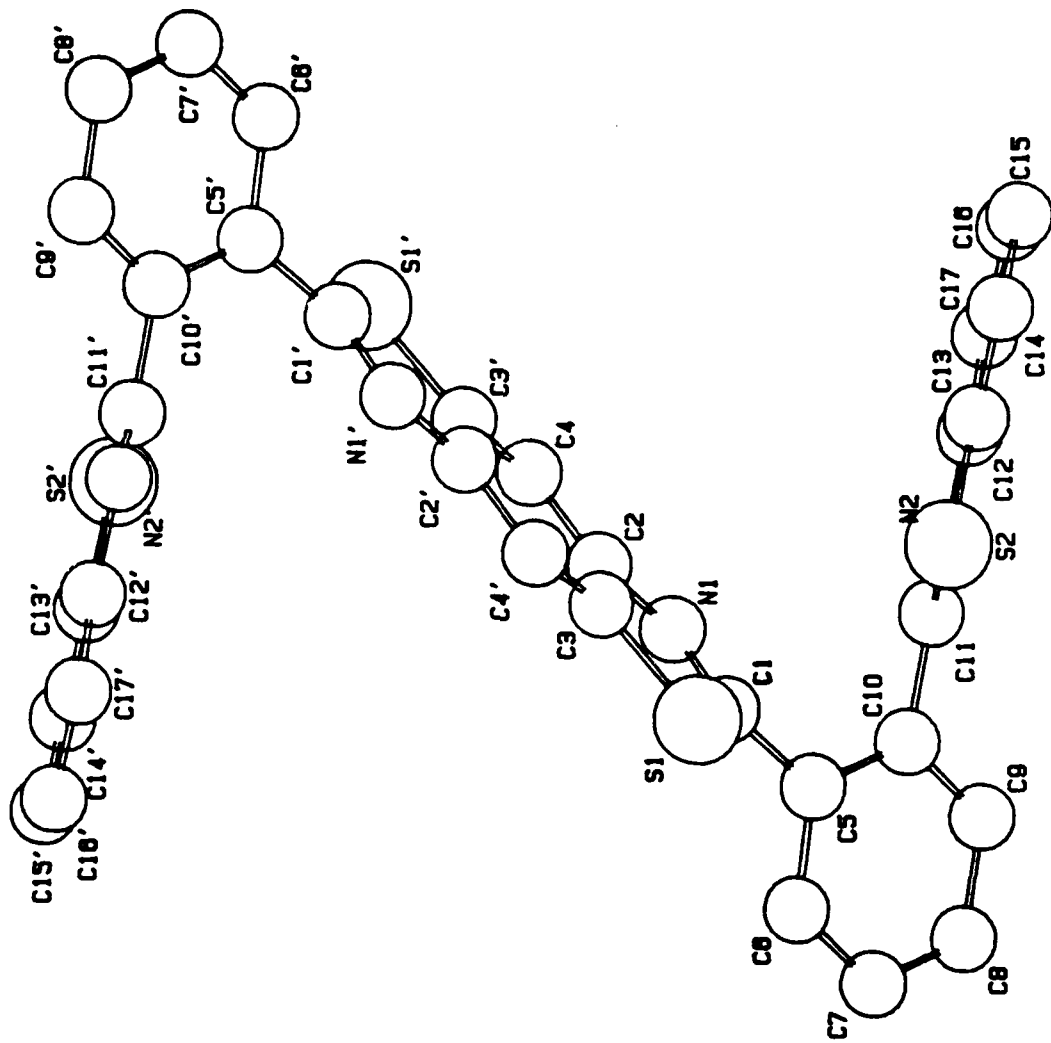


Table of Positional Parameters and Their Estimated Standard Deviations

Atom	x	y	z	B(A ²)
O1	0.4839(4)	0.2744(3)	-0.0456(2)	3.58(5)
N1	0.5732(4)	0.1539(3)	-0.1858(2)	2.52(5)
N2	0.4306(5)	-0.1578(3)	-0.2058(2)	3.88(6)
N3	0.1330(4)	-0.0739(3)	-0.2854(2)	2.65(5)
C1	0.2132(5)	0.0744(3)	-0.0492(2)	1.98(5)
C2	0.1229(5)	-0.0327(3)	-0.0983(2)	2.00(5)
C3	-0.0878(5)	-0.1029(3)	-0.0491(2)	2.13(6)
C7	0.4264(5)	0.1647(3)	-0.0950(2)	2.41(6)
C8	0.6884(5)	0.3386(3)	-0.1096(2)	2.44(6)
C9	0.8242(6)	0.4549(4)	-0.0953(3)	3.29(7)
C10	1.0234(6)	0.4933(4)	-0.1724(3)	3.69(8)
C11	1.0824(6)	0.4186(4)	-0.2598(3)	3.85(8)
C12	0.9443(6)	0.3028(4)	-0.2741(3)	3.57(7)
C13	0.7445(5)	0.2639(3)	-0.1961(2)	2.57(6)
C14	0.2366(5)	-0.0826(3)	-0.1998(2)	2.26(6)
C15	0.4639(5)	-0.1999(4)	-0.3081(2)	3.05(6)
C16	0.6361(6)	-0.2833(5)	-0.3578(3)	5.20(9)
C17	0.6135(7)	-0.3071(4)	-0.4603(3)	4.30(8)
C18	0.4337(8)	-0.2501(4)	-0.5106(3)	4.29(9)
C19	0.2637(7)	-0.1685(4)	-0.4608(3)	4.95(9)
C20	0.2808(6)	-0.1460(3)	-0.3564(2)	2.69(6)

Anisotropically refined atoms are given in the form of the isotropic equivalent displacement parameter defined as:
 $(4/3) * [a^2 * B(1,1) + b^2 * B(2,2) + c^2 * B(3,3) + ab(\cos \gamma) * B(1,2) + ac(\cos \beta) * B(1,3) + bc(\cos \alpha) * B(2,3)]$

Table 2

Table of General Displacement Parameter Expressions - U's

Name	U(1,1)	U(2,2)	U(3,3)	U(1,2)	U(1,3)	U(2,3)
O1	0.037(1)	0.049(1)	0.050(1)	-0.010(1)	0.005(1)	-0.0193(9)
N1	0.028(1)	0.033(1)	0.031(1)	-0.006(1)	0.008(1)	-0.0106(9)
N2	0.035(1)	0.085(2)	0.042(1)	0.019(1)	-0.009(1)	-0.043(1)
N3	0.032(1)	0.046(1)	0.033(1)	0.013(1)	-0.011(1)	-0.0259(8)
C1	0.022(1)	0.026(1)	0.025(1)	-0.004(1)	0.002(1)	-0.0065(9)
C2	0.024(1)	0.028(1)	0.024(1)	0.000(1)	-0.000(1)	-0.0099(9)
C3	0.025(1)	0.030(1)	0.029(1)	-0.001(1)	-0.002(1)	-0.0144(9)
C7	0.026(1)	0.027(1)	0.038(1)	-0.002(1)	-0.004(1)	-0.008(1)
C8	0.024(1)	0.031(1)	0.035(1)	-0.003(1)	0.002(1)	-0.007(1)
C9	0.042(2)	0.039(1)	0.042(1)	-0.013(1)	0.004(1)	-0.014(1)
C10	0.041(2)	0.039(2)	0.052(2)	-0.015(2)	0.004(2)	-0.005(1)
C11	0.037(2)	0.043(2)	0.055(2)	-0.011(2)	0.014(2)	-0.008(1)
C12	0.044(2)	0.039(2)	0.043(2)	-0.003(2)	0.016(2)	-0.010(1)
C13	0.032(2)	0.029(1)	0.031(1)	-0.002(1)	0.005(1)	-0.006(1)
C14	0.056(1)	0.030(1)	0.031(1)	-0.004(1)	0.002(1)	-0.013(1)
C15	0.029(2)	0.056(2)	0.035(1)	-0.005(1)	0.004(1)	-0.026(1)
C16	0.040(2)	0.114(2)	0.062(2)	0.022(2)	-0.007(2)	-0.058(1)
C17	0.048(2)	0.073(2)	0.046(1)	-0.002(2)	0.011(2)	-0.037(1)
C18	0.082(3)	0.054(2)	0.030(1)	0.000(2)	-0.000(2)	-0.022(1)
C19	0.090(3)	0.070(2)	0.043(1)	0.027(2)	-0.028(2)	-0.033(1)
C20	0.041(2)	0.033(1)	0.029(1)	0.000(1)	-0.002(1)	-0.013(1)

The form of the anisotropic displacement parameter is:
 $\exp[-2\pi i2(h2a2U(1,1) + k2b2U(2,2) + l2c2U(3,3) + 2hkabU(1,2) + 2hlabU(1,3) + 2kibcU(2,3))]$ where a, b, and c are reciprocal lattice constants.

Table 3

Table of Bond Distances in Angstroms

Atom 1 =====	Atom 2 =====	Distance =====	Atom 1 =====	Atom 2 =====	Distance =====
O1	C7	1.347(4)	C8	C9	1.384(5)
O1	C8	1.385(3)	C8	C13	1.389(4)
N1	C7	1.329(4)	C9	C10	1.384(4)
N1	C13	1.392(5)	C10	C11	1.400(5)
N2	C14	1.319(5)	C11	C12	1.391(5)
N2	C15	1.401(4)	C12	C13	1.393(4)
N3	C14	1.321(4)	C15	C16	1.391(6)
N3	C20	1.393(4)	C15	C20	1.364(5)
C1	C2	1.412(4)	C16	C17	1.384(6)
C1	C7	1.466(4)	C17	C18	1.365(6)
C2	C3	1.390(4)	C18	C19	1.374(6)
C2	C14	1.490(4)	C19	C20	1.394(5)

Numbers in parentheses are estimated standard deviations in the least significant digits.

Table 4

Table of Bond Angles in Degrees

Atom 1	Atom 2	Atom 3	Angle	Atom 1	Atom 2	Atom 3	Angle
C7	O1	C8	105.0(2)	C11	C12	C13	116.4(3)
C7	N1	C13	105.0(3)	N1	C13	C8	108.1(2)
C14	N2	C15	105.7(3)	N1	C13	C12	130.9(4)
C14	N3	C20	104.3(2)	C8	C13	C12	121.0(4)
C2	C1	C7	125.4(2)	N2	C14	N3	114.4(3)
C1	C2	C3	119.1(2)	N2	C14	C2	123.8(3)
C1	C2	C14	125.7(2)	N3	C14	C2	121.3(3)
C3	C2	C14	115.2(3)	N2	C15	C16	131.5(3)
O1	C7	N1	114.2(2)	N2	C15	C20	106.3(3)
O1	C7	C1	119.5(2)	C16	C15	C20	122.2(3)
N1	C7	C1	126.3(3)	C15	C16	C17	116.3(3)
O1	C8	C9	129.3(3)	C16	C17	C18	121.8(3)
O1	C8	C13	107.9(3)	C17	C18	C19	121.6(3)
C9	C8	C13	122.9(3)	C18	C19	C20	117.6(4)
C8	C9	C10	116.3(3)	N3	C20	C15	109.4(3)
C9	C10	C11	121.5(3)	N3	C20	C19	130.2(3)
C10	C11	C12	121.9(3)	C15	C20	C19	120.5(3)

Numbers in parentheses are estimated standard deviations in the least significant digits.

Table 5

Table of Torsion Angles in Degrees

Preprint 1

Atom 1 =====	Atom 2 =====	Atom 3 =====	Atom 4 =====	Angle =====
C8	O1	C7	N1	-0.94 (0.32)
C8	O1	C7	C1	-178.93 (0.25)
C7	O1	C8	C9	-179.13 (0.31)
C7	O1	C8	C13	0.32 (0.31)
C13	N1	C7	O1	1.15 (0.33)
C13	N1	C7	C1	178.98 (0.28)
C7	N1	C13	C8	-0.88 (0.32)
C7	N1	C13	C12	178.70 (0.33)
C15	N2	C14	N3	1.87 (0.35)
C15	N2	C14	C2	172.91 (0.27)
C14	N2	C15	C16	-178.57 (0.36)
C14	N2	C15	C20	-0.43 (0.34)
C20	N3	C14	N2	-2.46 (0.34)
C20	N3	C14	C2	-173.76 (0.25)
C14	N3	C20	C15	2.06 (0.32)
C14	N3	C20	C19	-178.53 (0.34)
C7	C1	C2	C3	-176.3 (0.26)
C7	C1	C2	C14	5.22 (0.45)
C2	C1	C7	O1	173.91 (0.26)
C2	C1	C7	N1	-3.81 (0.47)
C1	C2	C14	N2	60.42 (0.41)
C1	C2	C14	N3	-129.13 (0.31)
C3	C2	C14	N2	-118.20 (0.33)
C3	C2	C14	N3	52.25 (0.36)
O1	C8	C9	C10	178.91 (0.30)
C13	C8	C9	C10	-0.47 (0.47)
O1	C8	C13	N1	0.35 (0.33)
O1	C8	C13	C12	-179.28 (0.28)
C9	C8	C13	N1	179.84 (0.30)
C9	C8	C13	C12	0.21 (0.47)
C8	C9	C10	C11	0.25 (0.50)
C9	C10	C11	C12	0.23 (0.54)
C10	C11	C12	C13	-0.49 (0.50)
C11	C12	C13	N1	-179.26 (0.31)
C11	C12	C13	C8	0.27 (0.47)
N2	C15	C16	C17	178.68 (0.34)
C20	C15	C16	C17	0.79 (0.53)
N2	C15	C20	N3	-1.03 (0.34)
N2	C15	C20	C19	179.50 (0.30)
C16	C15	C20	N3	177.33 (0.31)
C16	C15	C20	C19	-2.14 (0.51)
C15	C16	C17	C18	0.89 (0.56)
C16	C17	C18	C19	-1.23 (0.59)
C17	C18	C19	C20	-0.12 (0.57)
C18	C19	C20	N3	-177.58 (0.32)
C18	C19	C20	C15	1.77 (0.51)

Table 6

Table of Positional Parameters and Their Estimated Standard Deviations

Atom	x	y	z	B(A ²)
S1	0.3610(2)	0.0335(2)	0.2123(2)	4.41(6)
S2	0.1535(2)	-0.0576(2)	0.2331(2)	6.21(8)
N1	0.3822(4)	-0.1110(4)	0.3104(6)	3.3(2)
N2	0.1573(4)	-0.2259(5)	0.2316(5)	4.2
C1	0.3358(5)	-0.0710(5)	0.2041(7)	3.3(2)
C2	0.4436(5)	-0.0585(5)	0.4106(6)	3.2(2)
C3	0.4422(5)	0.0233(5)	0.3743(6)	3.1(2)
C4	0.4975(6)	0.0833(5)	0.4618(7)	3.7(2)
C5	0.2634(6)	-0.1088(5)	0.0826(7)	3.3(2)
C6	0.2751(6)	-0.1049(7)	-0.0225(8)	4.8(3)
C7	0.2125(7)	-0.1454(7)	-0.1341(8)	5.5(3)
C8	0.1393(7)	-0.1924(6)	-0.1422(8)	5.1(3)
C9	0.1250(6)	-0.1941(6)	-0.0400(7)	4.4(3)
C10	0.1868(5)	-0.1533(5)	0.0723(7)	3.3(2)
C11	0.1671(5)	-0.1528(6)	0.1801(7)	4.0(2)
C12	0.1378(5)	-0.1918(6)	0.3248(7)	3.7(2)
C13	0.1325(5)	-0.1082(6)	0.3383(7)	4.1(2)
C14	0.1119(6)	-0.0741(6)	0.4264(9)	5.2(3)
C15	0.0992(6)	-0.1276(7)	0.5023(7)	5.0(3)
C16	0.1079(7)	-0.2094(6)	0.4965(9)	5.0(3)
C17	0.1263(7)	-0.2430(6)	0.4089(9)	5.5(3)

Anisotropically refined atoms are given in the form of the isotropic equivalent displacement parameter defined as:
 $(4/3) * [a^2 * B(1,1) + b^2 * B(2,2) + c^2 * B(3,3) + ab(\cos \gamma) * B(1,2) + ac(\cos \beta) * B(1,3) + bc(\cos \alpha) * B(2,3)]$

Table 7

Table of General Displacement Parameter Expressions - U's

Name	U(1,1)	U(2,2)	U(3,3)	U(1,2)	U(1,3)	U(2,3)
S1	0.062(1)	0.054(1)	0.0433(9)	-0.014(1)	0.0212(7)	0.005(1)
S2	0.096(1)	0.078(2)	0.077(1)	-0.004(2)	0.0567(8)	-0.001(2)
N1	0.049(3)	0.037(4)	0.038(3)	-0.015(3)	0.022(2)	-0.008(3)
N2	0	0	0	0	0	0
C1	0.043(4)	0.052(6)	0.039(3)	-0.003(4)	0.026(2)	0.007(4)
C2	0.045(3)	0.043(5)	0.043(3)	-0.010(4)	0.030(2)	-0.002(4)
C3	0.045(4)	0.045(5)	0.035(3)	-0.008(4)	0.024(2)	0.001(4)
C4	0.060(4)	0.036(5)	0.052(4)	-0.009(4)	0.035(3)	0.005(4)
C5	0.046(4)	0.045(6)	0.033(3)	0.004(4)	0.019(2)	-0.001(4)
C6	0.054(4)	0.077(7)	0.056(4)	-0.003(5)	0.033(3)	0.001(5)
C7	0.082(5)	0.086(8)	0.046(4)	0.011(6)	0.037(3)	-0.002(5)
C8	0.068(5)	0.073(7)	0.042(4)	-0.006(6)	0.021(3)	-0.006(5)
C9	0.056(5)	0.062(7)	0.052(4)	-0.008(5)	0.030(3)	-0.004(4)
C10	0.044(4)	0.045(5)	0.042(3)	-0.008(4)	0.025(2)	-0.004(4)
C11	0.031(4)	0.073(7)	0.046(4)	-0.015(4)	0.020(2)	-0.013(4)
C12	0.041(4)	0.057(6)	0.045(4)	-0.019(4)	0.024(2)	0.003(4)
C13	0.043(4)	0.059(6)	0.052(4)	-0.012(4)	0.024(3)	0.019(4)
C14	0.068(5)	0.053(6)	0.076(5)	-0.005(5)	0.039(3)	-0.009(5)
C15	0.067(4)	0.088(7)	0.051(4)	-0.029(5)	0.040(3)	-0.025(5)
C16	0.076(5)	0.054(6)	0.066(4)	-0.017(5)	0.040(3)	-0.002(5)
C17	0.072(5)	0.065(7)	0.077(5)	-0.016(5)	0.043(3)	-0.028(5)

The form of the anisotropic displacement parameter is:
 $\exp[-2\pi i^2(h^2a^2U(1,1) + k^2b^2U(2,2) + l^2c^2U(3,3) + 2hkabU(1,2) + 2hlacU(1,3) + 2klbcU(2,3))]$ where a, b, and c are reciprocal lattice constants.

Table 8

Table of Bond Distances in Angstroms

Atom 1 =====	Atom 2 =====	Distance =====	Atom 1 =====	Atom 2 =====	Distance =====
S1	C1	1.747(9)	C5	C10	1.40(1)
S1	C3	1.724(6)	C6	C7	1.38(1)
S2	C11	1.74(2)	C7	C8	1.38(2)
S2	C13	1.71(2)	C8	C9	1.39(2)
N1	C1	1.290(9)	C9	C10	1.39(2)
N1	C2	1.401(9)	C10	C11	1.51(1)
N2	C11	1.40(1)	C12	C13	1.38(1)
N2	C12	1.45(1)	C12	C17	1.41(2)
C1	C5	1.468(9)	C13	C14	1.40(2)
C2	C3	1.40(1)	C14	C15	1.37(2)
C3	C4	1.38(2)	C15	C16	1.36(1)
C5	C6	1.40(2)	C16	C17	1.38(2)

 Numbers in parentheses are estimated standard deviations in the least significant digits.

Table 9

Table of Bond Angles in Degrees

Atom 1	Atom 2	Atom 3	Angle	Atom 1	Atom 2	Atom 3	Angle
C1	S1	C3	89.4(4)	C8	C9	C10	120.5(9)
C11	S2	C13	88.0(5)	C5	C10	C9	120(1)
C1	N1	C2	110.4(7)	C5	C10	C11	120.6(7)
C11	N2	C12	98.7(7)	C9	C10	C11	119.5(8)
S1	C1	N1	116.1(5)	S2	C11	N2	121.7(8)
S1	C1	C5	120.7(6)	S2	C11	C10	117.2(7)
N1	C1	C5	123.3(8)	N2	C11	C10	121.1(8)
N1	C2	C3	114.8(6)	N2	C12	C13	121.8(9)
S1	C3	C2	109.3(6)	N2	C12	C17	121.1(8)
S1	C3	C4	128.5(7)	C13	C13	C17	117.1(9)
C2	C3	C4	122.2(7)	S2	C13	C12	109.8(8)
C1	C5	C6	119.3(8)	S2	C13	C14	127.7(8)
C1	C5	C10	121.4(8)	C12	C13	C14	122.6(9)
C6	C5	C10	119.3(7)	C13	C14	C15	116.9(9)
C5	C6	C7	120(1)	C14	C15	C16	123(2)
C6	C7	C8	120(2)	C15	C16	C17	121(2)
C7	C8	C9	119.7(8)	C12	C17	C16	120.1(9)

Numbers in parentheses are estimated standard deviations in the least significant digits.

Table of Torsion Angles in Degrees

Atom 1 =====	Atom 2 =====	Atom 3 =====	Atom 4 =====	Angle =====
C3	S1	C1	N1	0.09 (0.78)
C3	S1	C1	C5	178.32 (0.79)
C1	S1	C3	C2	-0.55 (0.70)
C1	S1	C3	C4	-178.59 (0.93)
C13	S2	C11	N2	0.48 (0.75)
C13	S2	C11	C10	178.40 (0.72)
C11	S2	C13	C12	0.10 (0.68)
C11	S2	C13	C14	-179.29 (0.94)
C2	N1	C1	S1	0.41 (1.02)
C2	N1	C1	C5	-177.78 (0.84)
C1	N1	C2	C3	-0.86 (1.12)
C12	N2	C11	S2	-0.81 (0.84)
C12	N2	C11	C10	-178.65 (0.77)
C11	N2	C12	C13	0.91 (1.00)
C11	N2	C12	C17	-177.03 (0.86)
S1	C1	C5	C6	59.40 (1.14)
S1	C1	C5	C10	-125.06 (0.81)
N1	C1	C5	C6	-122.49 (1.02)
N1	C1	C5	C10	53.05 (1.32)
N1	C2	C3	S1	0.91 (1.00)
N1	C2	C3	C4	179.10 (0.85)
C1	C5	C6	C7	174.76 (0.92)
C10	C5	C6	C7	-0.87 (1.46)
C1	C5	C10	C9	-174.17 (0.84)
C1	C5	C10	C11	9.67 (1.29)
C6	C5	C10	C9	1.36 (1.34)
C6	C5	C10	C11	-174.80 (0.86)
C5	C6	C7	C8	-2.07 (1.61)
C6	C7	C8	C9	4.50 (1.61)
C7	C8	C9	C10	-4.01 (1.52)
C8	C9	C10	C5	1.08 (1.40)
C8	C9	C10	C11	177.28 (0.89)
C5	C10	C11	S2	54.46 (1.04)
C5	C10	C11	N2	-127.61 (0.89)
C9	C10	C11	S2	-121.71 (0.83)
C9	C10	C11	N2	56.23 (1.18)
N2	C12	C13	S2	-0.67 (1.06)
N2	C12	C13	C14	178.76 (0.83)
C17	C12	C13	S2	177.34 (0.74)
C17	C12	C13	C14	-3.23 (1.38)
N2	C12	C17	C16	179.92 (0.90)
C13	C12	C17	C16	1.89 (1.46)
S2	C13	C14	C15	-179.06 (0.76)
C12	C13	C14	C15	1.62 (1.44)
C13	C14	C15	C16	1.47 (1.52)
C14	C15	C16	C17	-2.78 (1.65)
C15	C16	C17	C12	1.01 (1.64)

CUMULATIVE LIST OF PUBLICATIONS

1. "Model Compound Studies of Rigid Rod Aromatic Heterocyclic Polymer Systems: The X-Ray Crystal Structure of 2,6-Diphenylbenzo(1,2-d:5,4-d')diimidazobenzene Tetrahydrate, $C_{20}H_{14}N_4 \cdot 4H_2O$, A Model System for the Study of Polymer- H_2O Interaction in Polybenzimidazoles," M. Hunsaker, W.W. Adams and A.V. Fratini, Air Force Tech. Report AFWAL-TR-83-4055, July 1983.
2. " ^{13}C NMR and X-Ray Crystallographic Determination of the Structures of Some Isomeric Phenylquinoxalines," F. Hedberg, D. Bush, M. Ryan, R. Harvey, A. Fratini, D. Dudis, M. Barfield, S. Walter, D. Draney, and C. Marvel, Air Force Tech. Report AFWAL-TR-85-4037, 1985.
3. "The Structure of Poly-2,5-benzoxazole (ABPBO) and Poly-2,6-Benzothiazole (ABPBT) Fibers by X-Ray Diffraction," A.V. Fratini, E.M. Cross, J.F. O'Brien and W.W. Adams, Air Force Tech. Report AFWAL-TR-85-4097, July 1985.
4. "The Structure of Poly-2,5-benzoxazole (ABPBO) and Poly-2,6-benzothiazole (ABPBT) Fibers by X-Ray Diffraction," A.V. Fratini, E.M. Cross, J.F. O'Brien and W.W. Adams, J. Macromol. Sci. - Phys., B24(1-4), 159-179 (1985-1986).
5. "Refinement of the Structure of PEEK Fibre in an Orthorhombic Unit Cell," A.V. Fratini, E.M. Cross, R.B. Whitaker and W.W. Adams, Polymer, 27, 861-865 (1986).

6. "Fluoro-Ketones IX. Hydration of Perfluoroalkylpolyketones and their Reactions Forming Novel Cyclic Compounds," L.S. Chen, A.V. Fratini and C. Tamborski, J. Fluorine Chem., **31**, 381-393 (1986).
7. "Structure of a Dioxabicyclic Fluoro Octane Derivative," P.G. Lenhart and A.V. Fratini, Acta Cryst., **C43**, 1929-1932 (1987).

PROFESSIONAL PERSONNEL

1. Dr. A. V. Fratini, Principal Investigator, Professor of Chemistry, University of Dayton.
2. Dr. K. Baker, Postdoctoral Associate, University of Dayton.
3. Dr. H. Knachel, Professor of Chemistry, University of Dayton.
4. Mr. M. Anater, Undergraduate Student, University of Dayton.
5. Mr. G. Borchers, Undergraduate Student, University of Dayton.
6. Ms. E. Cross, Undergraduate Student, University of Dayton.
7. Mr. C. George, Undergraduate Student, University of Dayton.
8. Mr. J. Plashke, Undergraduate Student, University of Dayton.
9. Ms. M. Sturtevant, Undergraduate Student, University of Dayton.

PRESENTATIONS

1. Paper (Abstract 1) was presented at the Annual Meeting of the American Crystallographic Association, Stanford University, Stanford, California, August 18-29, 1985.
2. Paper (Abstract 2) was presented at the National Meeting of the American Physical Society, High Polymer Physics Division, Detroit, Michigan, March 25-29, 1985.
3. Much of this work has been presented at the regularly scheduled Reviews of the Air Force Ordered Polymer Research Program, organized by Dr. T. Helminiak and held in Dayton, Ohio.

4. Presentations have also been given at two DARPA/DSO-AFOSR/NC Optical Processing Annual Reviews sponsored by EDM Corporation, McLean Va., Nov. 1984 and Nov. 1985.

DATE
FILMED
58